ISSN 0915-633X

NATIONAL INSTITUTE FOR FUSION SCIENCE

Direct-interaction Approximation and Reynolds-number Reversed Expansion for a Dynamical System

S. Goto and S. Kida

(Received - June 13, 1997)

NIFS-499 July 1997

RESEARCH REPORT
NIFS Series

NAGOYA, JAPAN

Direct-interaction approximation and Reynolds-number reversed expansion for a dynamical system

Susumu GOTO [a] and Shigeo KIDA [b]

[a] *School of Mathematical and Physical Science, The Graduate University for Advanced Studies, Oroshi-cho 322-6, Toki-shi, 509-52, Japan*
[b] *National Institute for Fusion Science, Oroshi-cho 322-6, Toki-shi, 509-52, Japan*

Abstract

The condition of validity of the direct-interaction approximation and the Reynolds-number reversed expansion truncated at the lowest nontrivial order is assessed numerically for a dynamical system composed of coupled equations of many variables with quadratic-nonlinear terms of weak or strong coupling as well as linear-viscous and randomly forcing terms. Although these two theories lead to an identical set of integro-differential equations for the correlation function of the dependent variables and the response function, their parameter regions of validity are different from each other. The direct-interaction approximation works well for larger number of degrees of freedom if the nonlinear couplings are as weak as the Navier-Stokes equation, but not when the nonlinear coupling is strong. The Reynolds-number reversed expansion, on the other hand, works well whenever the nonlinear term is smaller in magnitude than the other terms irrespective of the strength of the nonlinear coupling.

Keywords: Direct-interaction approximation; Dynamical system; Turbulence

1 Introduction

The direct-interaction approximation (DIA) was originally introduced and applied to incompressible isotropic homogeneous turbulence by Kraichnan [1]. This is an approximation without neglecting the nonlinearity of the basic equation, and without introducing any *ad hoc* adjustable parameters. Lagrangian versions of DIA [2–4] give excellent predictions for various statistical quantities such as the Kolmogorov universal form of the energy spectrum function and the skewness of the velocity gradient. It is an interesting observation that a set of integro-differential equations for the Eulerian velocity correlation and the response functions derived by DIA [1] are also obtained by different kinds of approximations. For example, they are rederived by diagrammatic techniques developed by Wyld [5] and Martin *et al.* [6], and also by a method described in Leslie's textbook [7] as an explanation of DIA, which is a Reynolds-number expansion followed by a formal replacement of variables. This last method was justified in ref. [8] by a kind of systematic expansion, which we call here the Reynolds-number reversed expansion (RRE). It was shown in ref. [8] that the Lagrangian-history DIA and the abridged-Lagrangian-history DIA [2] equations can be also derived by this expansion. It should be noted, however, that DIA and RRE are based upon completely different ideas and procedures though they lead to a same set of final equations. In fact, as shown in the present paper, each theory has different parameter region of applicability. Obviously, RRE should work for small Reynolds numbers, i.e., for weak nonlinearity. For DIA, on the other hand, no systematic studies have ever been made to clarify its applicability, which we investigate and discuss in this paper.

In order to make it easier to survey a wide range of parameters we deal with a dynamical system which is simpler than the Navier-Stokes equation but still retains important ingredients of the latter, that is, quadratic-nonlinear and linear-viscous terms. A random force is imposed to prevent the solutions from decaying. This system is different from several typical models studied before to check statistical theories of turbulence and to discuss the characteristics of turbulence [9–12]. Our model equation is introduced and solved numerically as an initial value problem in §2. It turns out that the strength of nonlinear coupling is important for the DIA formulation. A case of weak nonlinear coupling, for which DIA works well, is simulated in this section. (It will be shown in §5.3 that DIA is not applicable to a case of strong nonlinear coupling.) Then, DIA and RRE are formulated in §§3 and 4, respectively. It is stressed that the largeness of the degrees of freedom and the weakness of the nonlinear coupling are prerequisite in the derivation of the integro-differential equations by DIA. Validity of all the working assumptions introduced in DIA is confirmed numerically in §5. Further discussions on the difference between the two theories and their validity are provided in §6.

2 Model equation

We consider the temporal evolution of a set of N real variables X_i ($i = 1, 2, \cdots, N$) governed by

$$\frac{\mathrm{d}}{\mathrm{d}t} X_i(t) = \sum_j \sum_k C_{ijk}\, X_j(t)\, X_k(t) - \nu_i\, X_i(t) + F_i(t) \qquad (i = 1, 2, \cdots, N)\ , \tag{2.1}$$

where $\sum_i$ stands for $\sum_{i=1}^{N}$. (The summation convention for repeated subscripts are not used throughout this paper.) The coefficient, ν_i, of the linear term is a positive constant, which is an analogue of the viscous effect in the Fourier representation of the Navier-Stokes equation. It can be assumed, without loss of generality, that the time-independent coefficients, C_{ijk}, of the quadratic-nonlinear terms should be symmetric with respect to the second and the third subscripts, i.e.,

$$C_{ijk} = C_{ikj}\ . \tag{2.2}$$

We further assume that

$$C_{ijk} + C_{jki} + C_{kij} = 0 \tag{2.3}$$

so that the sum of the energy of three modes $\frac{1}{2}\,(X_i^2 + X_j^2 + X_k^2)$ may not change through the direct interaction among them. This property of detailed balance of energy is analogous to the Navier-Stokes system, and guarantees the conservation of the total energy of the system $\mathcal{E} = \frac{1}{2}\sum_i X_i^2$ when the viscosity ν (and therefore F_i, see (2.4) below) vanishes. There is still an arbitrariness in the choice of the numerical values of the coefficients with the above properties. Concrete examples will be given in the subsequent sections (§§2.1 and 5.3). Here, notice that model equation (2.1) can be equivalent to a forced Navier-Stokes equation if coefficients C_{ijk} and ν_i are appropriately chosen (cf. (6.1)). In the following we put $\nu_i = \nu$ for simplicity.

The inhomogeneous term $F_i(t)$ is a random driving force. It is piecewise constant in each time interval Δt, which is set to be equal to the time increment of the numerical simulations, and the amplitude obeys a Gaussian distribution of zero mean and of variance given by

$$\sigma^2 = \frac{2\,\nu}{N \Delta t}\ . \tag{2.4}$$

The forcing at different time intervals or of different modes are assumed to be statistically independent of each other. Variance (2.4) has been chosen so that the averaged total energy be a half of unity

$$\overline{\mathcal{E}} = \frac{1}{2} \sum_i \overline{X_i^2} = \frac{1}{2} \tag{2.5}$$

in the statistically stationary state [1]. The overbar stands for an ensemble average (or a long-term average in a single run of the simulation).

[1] By taking an ensemble average of equation (2.1) multiplied by X_i and summed up over $1 \le i \le N$, we obtain the energy equation as

$$\nu \sum_i \overline{X_i^2} = \sum_i \overline{F_i X_i} = \frac{N}{2}\,\sigma^2\,\Delta t\ ,$$

in the statistically stationary state.

N	(a_n, b_n, c_n)
7	$(1,2,4)$
10	$(1,2,7)$
20	$(1,2,17),(4,5,11)$
40	$(1,2,37),(4,5,31),(6,7,27),(8,10,22),(11,12,17)$

Table.1. Triplets (a_n, b_n, c_n) adopted in the present numerical simulation.

2.1 Direct numerical simulation

Before going to the formulation of the closure equations, it may be useful to see the statistical property of model equation (2.1). We solve it numerically as the initial value problem. The coefficients C_{ijk} are specified by the following two steps. First, those coefficients of which any two subscripts are identical are put zero, namely,

$$C_{ijk} = 0 \qquad (\text{if } i = j \text{ or } j = k \text{ or } k = i)\ . \tag{2.6}$$

Next, we take a circle of circumference N and assign N points with equal distance apart on it (Fig.1). For any triplets of integers, i, j and k, we introduce a, b and c as three arc lengths divided by these three points in such a way that the point i is sandwiched by a and c, and that a, b and c are placed counterclockwise. Here, we choose a series of triplets of natural numbers $(a_n,\ b_n,\ c_n)$ $(a_n + b_n + c_n = N;\ n = 1,2,3,\cdots)$ so that there is no common element in a set $\{x | x = a_n, b_n, c_n, N - a_n, N - b_n, N - c_n;\ n = 1,2,3,\cdots\}$ [2] . The coefficients C_{ijk} are then defined by

$$C_{ijk} = \begin{cases} \frac{1}{3}N - b & (\text{ if } \exists n \text{ such that } (a,b,c) \equiv (a_n, b_n, c_n)\ )\ , \qquad (2.7a) \\ 0 & (\text{ otherwise }),\qquad (2.7b) \end{cases}$$

where $(a,b,c) \equiv (a',b',c')$ implies that (a,b,c) is equal to (a',b',c') itself or its cyclic permutation. The coefficients thus determined guarantees that [I] C_{ijk} satisfies conditions (2.2) and (2.3), [II] the system is symmetric with respect to i and [III] there is only a single, at the most, direct interaction between each pair of modes $\{X_i\}$. The last property (weak coupling) may be reminiscent of the triad interaction among the Fourier components of the velocity in the Navier-Stokes equation, which is essential in the formulation of DIA (see §§5.3 and 6).

The initial values of X_i are given by random numbers under the constraint that $\sum_i X_i^2 = 1$. The fourth-order Runge-Kutta scheme is employed for the time integration. There are two control parameters which

[2] The choice of a_n, b_n and c_n is not unique, and one adopted in the present paper is shown in Table.1.

characterize the present system, that is, the degrees of freedom N and the viscosity ν. In order to examine the dependence of the statistics of the system on these parameters we perform two series of simulations; $(N,\nu) = (7,100),(7,10),(7,1),(7,0)$ and $(N,\nu) = (7,0),(10,0),(20,0),(40,0)$. In the first series we examine the viscosity dependence, while in the second the dependence on the numbers of degrees of freedom. The time increment Δt is taken as 5×10^{-3}, 2×10^{-3}, 10^{-3} and 10^{-4} for $N = 7$, 10, 20 and 40, respectively.

2.2 Correlation function

The two-time two-mode correlation function

$$V_{in}(t,t') = \overline{X_i(t)\,X_n(t')} \qquad (t \geq t') \tag{2.8}$$

is one of the representative statistical quantities which characterize the dynamical system (2.1). The governing equations for it are derived from (2.1) as

$$\left[\frac{\partial}{\partial t} + \nu\right] V_{in}(t,t') = \sum_j \sum_k C_{ijk}\,\overline{X_j(t)\,X_k(t)\,X_n(t')} \qquad (t > t') \tag{2.9}$$

and

$$\left[\frac{\mathrm{d}}{\mathrm{d}t} + 2\nu\right] V_{in}(t,t) = \sum_j \sum_k C_{ijk}\,\overline{X_j(t)\,X_k(t)\,X_n(t)} + \overline{F_i(t)\,X_n(t)} + (i \leftrightarrow n)\,. \tag{2.10}$$

These equations cannot be solved because of the appearance of a higher-order (third-order) correlation function which originates from the nonlinearity of (2.1). This is the well-known closure problem. As closure theories to solve it, we consider DIA in §3 and RRE in §4.

For a later comparison with the statistical theories we show here the the auto-correlation function ($i = n$) obtained by the numerical simulations described in the preceding subsection. The viscosity dependence of the auto-correlation function is depicted in Fig.2(a) in which those for $\nu = 0$, 1, 10 and 100 are compared in the case of $N = 7$. The time is normalized by the viscous time-scale $1/\nu$ in Fig.2(b) (see (2.9)). We see that the characteristic time-scale of the velocity auto-correlation function changes in proportion to the viscous time for $\nu \gg 1$.

In Fig.3(a) we show the dependence on the number of degrees of freedom of the auto-correlation function, where those for $N = 7$, 10, 20 and 40 are compared in the inviscid case. The decaying time-scale of the function decreases as N increases. The time is normalized by the times-scale $\sqrt{N/c_1}$ of the nonlinear term in Fig.3(b) (see the paragraph below (5.9)).

3 Direct-interaction approximation

In this section we deal with DIA. For later use, we introduce a response function of X_i

$$G_{in}(t|t') = \frac{\delta X_i(t)}{\delta X_n(t')} \qquad (t \geq t')\,, \tag{3.1}$$

where δ stands for a functional derivative. The evolution equation of G_{in} is derived from (2.1), by taking a functional derivative with respect to $X_n(t')$, as

$$\frac{\partial}{\partial t} G_{in}(t|t') = \sum_j \sum_k 2\, C_{ijk}\, X_j(t)\, G_{kn}(t|t') - \nu\, G_{in}(t|t') \qquad (t > t') \,. \tag{3.2}$$

The boundary condition is given by

$$G_{in}(t|t) = \delta_{in} \,, \tag{3.3}$$

where δ_{in} denotes Kronecker's delta. In the following we derive a closed set of equations for V_{in} and $\overline{G}_{in}$ by the use of DIA from basic equation (2.1) and its products (2.9), (2.10), (3.2) and (3.3).

3.1 Direct-interaction decomposition

The DIA is formulated on the basis of the direct-interaction decomposition [1, 4], in which the true field X_i is decomposed into two fields, an NDI (Non-Direct-Interaction) field $X^{(0)}_{i/i_0j_0k_0}$ and a DI (Direct-Interaction) field $X^{(1)}_{i/i_0j_0k_0}$, as

$$X_i(t) = X^{(0)}_{i/i_0j_0k_0}(t|t_0) + X^{(1)}_{i/i_0j_0k_0}(t|t_0) \quad (t \geq t_0) \,. \tag{3.4}$$

Here, $X^{(0)}_{i/i_0j_0k_0}(t|t_0)$ $(t \geq t_0)$ is defined as a fictitious field without the direct interaction among three particular modes X_{i_0}, X_{j_0} and X_{k_0}, and t_0 denotes the time when the interaction is removed, i.e.,

$$X^{(0)}_{i/i_0j_0k_0}(t_0|t_0) = X_i(t_0) \qquad \text{and} \qquad X^{(1)}_{i/i_0j_0k_0}(t_0|t_0) = 0 \,. \tag{3.5}$$

For simplicity of notations, the argument t_0 in $X^{(0)}_{i/i_0j_0k_0}$ and $X^{(1)}_{i/i_0j_0k_0}$ will be omitted below. It follows from the definition that the NDI field obeys

$$\frac{\mathrm{d}}{\mathrm{d}t} X^{(0)}_{i/i_0j_0k_0}(t) = \sum_{\substack{j \\ \{i,j,k\} \neq \{i_0,j_0,k_0\}}} \sum_k C_{ijk}\, X^{(0)}_{j/i_0j_0k_0}(t)\, X^{(0)}_{k/i_0j_0k_0}(t) - \nu\, X^{(0)}_{i/i_0j_0k_0}(t) + F_i(t) \,. \tag{3.6}$$

Subtraction of the above equation from (2.1) leads to the equation for the DI field as

$$\begin{aligned} \frac{\mathrm{d}}{\mathrm{d}t} X^{(1)}_{i/i_0j_0k_0}(t) = & \sum_{\substack{j \\ \{i,j,k\} \neq \{i_0,j_0,k_0\}}} \sum_k 2\, C_{ijk}\, X_j(t)\, X^{(1)}_{k/i_0j_0k_0}(t) - \nu\, X^{(1)}_{i/i_0j_0k_0}(t) \\ & + 2\,\delta_{ii_0}\, C_{i_0j_0k_0}\, X^{(0)}_{j_0/i_0j_0k_0}(t)\, X^{(0)}_{k_0/i_0j_0k_0}(t) \\ & + 2\,\delta_{ij_0}\, C_{j_0k_0i_0}\, X^{(0)}_{k_0/i_0j_0k_0}(t)\, X^{(0)}_{i_0/i_0j_0k_0}(t) \\ & + 2\,\delta_{ik_0}\, C_{k_0i_0j_0}\, X^{(0)}_{i_0/i_0j_0k_0}(t)\, X^{(0)}_{j_0/i_0j_0k_0}(t) \,, \end{aligned} \tag{3.7}$$

where $X^{(1)}_i$ is assumed to be much smaller than $X^{(0)}_i$ in magnitude (see DIA assumption 1 below).

The response function G_{in} is similarly decomposed as

$$G_{in}(t|t') = G^{(0)}_{in/i_0j_0k_0}(t|t') + G^{(1)}_{in/i_0j_0k_0}(t|t') \,, \tag{3.8}$$

where $G^{(0)}_{in/i_0j_0k_0}$ is governed by

$$\frac{\partial}{\partial t} G^{(0)}_{in/i_0j_0k_0}(t|t') = \sum_{\substack{j \\ \{i,j,k\}\neq\{i_0,j_0,k_0\}}} \sum_{k} 2\,C_{ijk}\,X_j(t)\,G^{(0)}_{kn/i_0j_0k_0}(t|t') - \nu\,G^{(0)}_{in/i_0j_0k_0}(t|t')\ . \tag{3.9}$$

Here, the direct-interaction decomposition has been made at t'. The evolution equation for the DI field of the response function is, then, obtained from this equation and (3.2) as

$$\begin{aligned}
\frac{\partial}{\partial t} G^{(1)}_{in/i_0j_0k_0}(t|t') = & \sum_{\substack{j \\ \{i,j,k\}\neq\{i_0,j_0,k_0\}}} \sum_{k} 2\,C_{ijk}\,X_j(t)\,G^{(1)}_{kn/i_0j_0k_0}(t|t') - \nu\,G^{(1)}_{in/i_0j_0k_0}(t|t') \\
& + 2\,\delta_{ii_0}\,C_{i_0j_0k_0}\,X_{j_0}(t)\,G^{(0)}_{k_0n/i_0j_0k_0}(t|t') \\
& + 2\,\delta_{ii_0}\,C_{i_0j_0k_0}\,X_{k_0}(t)\,G^{(0)}_{j_0n/i_0j_0k_0}(t|t') \\
& + 2\,\delta_{ij_0}\,C_{j_0k_0i_0}\,X_{k_0}(t)\,G^{(0)}_{i_0n/i_0j_0k_0}(t|t') \\
& + 2\,\delta_{ij_0}\,C_{j_0k_0i_0}\,X_{i_0}(t)\,G^{(0)}_{k_0n/i_0j_0k_0}(t|t') \\
& + 2\,\delta_{ik_0}\,C_{k_0i_0j_0}\,X_{i_0}(t)\,G^{(0)}_{j_0n/i_0j_0k_0}(t|t') \\
& + 2\,\delta_{ik_0}\,C_{k_0i_0j_0}\,X_{j_0}(t)\,G^{(0)}_{i_0n/i_0j_0k_0}(t|t')\ ,
\end{aligned} \tag{3.10}$$

where we have assumed that $|G^{(1)}_{in/i_0j_0k_0}| \ll |G^{(0)}_{in/i_0j_0k_0}|$ (see DIA assumption 1 below). The boundary conditions are written, from (3.3), as

$$G^{(0)}_{in/i_0j_0k_0}(t|t) = \delta_{in} \qquad \text{and} \qquad G^{(1)}_{in/i_0j_0k_0}(t|t) = 0\ . \tag{3.11}$$

Then, it follows from (3.5), (3.7), (3.9) and (3.11) that

$$\begin{aligned}
X^{(1)}_{i/i_0j_0k_0}(t) = \int_{t_0}^{t} \mathrm{d}t' \Big[& 2\,G^{(0)}_{ii_0/i_0j_0k_0}(t|t')\,C_{i_0j_0k_0}\,X^{(0)}_{j_0/i_0j_0k_0}(t')\,X^{(0)}_{k_0/i_0j_0k_0}(t') \\
& + 2\,G^{(0)}_{ij_0/i_0j_0k_0}(t|t')\,C_{j_0k_0i_0}\,X^{(0)}_{k_0/i_0j_0k_0}(t')\,X^{(0)}_{i_0/i_0j_0k_0}(t') \\
& + 2\,G^{(0)}_{ik_0/i_0j_0k_0}(t|t')\,C_{k_0i_0j_0}\,X^{(0)}_{i_0/i_0j_0k_0}(t')\,X^{(0)}_{j_0/i_0j_0k_0}(t') \Big]\ ,
\end{aligned} \tag{3.12}$$

and, from (3.9)—(3.11), that

$$\begin{aligned}
G^{(1)}_{in/i_0j_0k_0}(t|t') = \int_{t'}^{t} \mathrm{d}t'' \Big[& 2\,G^{(0)}_{ii_0/i_0j_0k_0}(t|t'')\,C_{i_0j_0k_0}\,X_{j_0}(t'')\,G^{(0)}_{k_0n/i_0j_0k_0}(t''|t') \\
& + 2\,G^{(0)}_{ii_0/i_0j_0k_0}(t|t'')\,C_{i_0j_0k_0}\,X_{k_0}(t'')\,G^{(0)}_{j_0n/i_0j_0k_0}(t''|t') \\
& + 2\,G^{(0)}_{ij_0/i_0j_0k_0}(t|t'')\,C_{j_0k_0i_0}\,X_{k_0}(t'')\,G^{(0)}_{i_0n/i_0j_0k_0}(t''|t') \\
& + 2\,G^{(0)}_{ij_0/i_0j_0k_0}(t|t'')\,C_{j_0k_0i_0}\,X_{i_0}(t'')\,G^{(0)}_{k_0n/i_0j_0k_0}(t''|t') \\
& + 2\,G^{(0)}_{ik_0/i_0j_0k_0}(t|t'')\,C_{k_0i_0j_0}\,X_{i_0}(t'')\,G^{(0)}_{j_0n/i_0j_0k_0}(t''|t') \\
& + 2\,G^{(0)}_{ik_0/i_0j_0k_0}(t|t'')\,C_{k_0i_0j_0}\,X_{j_0}(t'')\,G^{(0)}_{i_0n/i_0j_0k_0}(t''|t') \Big]\ .
\end{aligned} \tag{3.13}$$

The DI fields $X^{(1)}_{i/i_0j_0k_0}$ and $G^{(1)}_{in/i_0j_0k_0}$ are thus expressed in terms of the NDI and the true fields.

Before proceeding further, we summarize the assumptions employed in DIA, which are

DIA assumption 1 The DI field $X^{(1)}_{i/i_0j_0k_0}$ (or $G^{(1)}_{in/i_0j_0k_0}$) is much smaller in magnitude than the NDI field $X^{(0)}_{i/i_0j_0k_0}$ (or $G^{(0)}_{in/i_0j_0k_0}$), over the period of order of the decaying time-scale of the auto-correlation function.

DIA assumption 2 (I) Three variables $X^{(0)}_{i/ijk}$, $X^{(0)}_{j/ijk}$ and $X^{(0)}_{k/ijk}$, among which the direct interaction is absent, are statistically independent of each other. (II) Similarly, $G^{(0)}_{in/ijk}$, $G^{(0)}_{jn/ijk}$ and X_k are statistically independent of each other.

These assumptions may be reasonably accepted if the degrees of freedom N of the system is large enough. Since there are a lot of direct interactions for $N \gg 1$, the influence of extracting only a single one should be negligible, and therefore the NDI field $X^{(0)}_i$ (or $G^{(0)}_{in}$) may approximate the true field X_i (or G_{in}), which is DIA assumption 1. DIA assumption 2 is based upon the idea that the correlation among three modes without direct interaction should be weak. This assumption may also be justified only in the case of $N \gg 1$. For example, the contribution to the dynamics of $X^{(0)}_{i_0/i_0j_0k_0}$ from $X^{(0)}_{j_0/i_0j_0k_0}$ or $X^{(0)}_{k_0/i_0j_0k_0}$ through the *indirect* interaction terms is not negligibly small unless $N \gg 1$. We will check in §5.2 the validity of these assumptions by making a comparison with direct numerical simulations.

3.2 Correlation function

The DIA is applied here to the governing equations (2.9) and (2.10) for the correlation functions. First, we consider the two-time correlation function. By substituting direct-interaction decomposition (3.4) into the nonlinear term of (2.9), we obtain

$$\begin{aligned}\sum_j \sum_k C_{ijk}\, \overline{X_j(t)\, X_k(t)\, X_n(t')} = &\sum_j \sum_k C_{ijk}\, \overline{X^{(0)}_{j/jkn}(t)\, X^{(0)}_{k/jkn}(t)\, X^{(0)}_{n/jkn}(t')} \\ &+ \sum_j \sum_k 2\, C_{ijk}\, \overline{X^{(0)}_{j/jkn}(t)\, X^{(1)}_{k/jkn}(t)\, X^{(0)}_{n/jkn}(t')} \\ &+ \sum_j \sum_k C_{ijk}\, \overline{X^{(0)}_{j/jkn}(t)\, X^{(0)}_{k/jkn}(t)\, X^{(1)}_{n/jkn}(t')}\,, \end{aligned} \tag{3.14}$$

where the higher-order terms of the DI field have been neglected under DIA assumption 1. Notice that a different triplet of (i_0, j_0, k_0) is chosen in each term in the summand of the right-hand side of the above equation, i.e., $(i_0, j_0, k_0) = (i, j, k)$.

Now we evaluate each term in the right-hand side of (3.14) in turn. It follows from DIA assumption 2(I) that

$$\text{(First term in r.h.s. of (3.14))} = 0\,. \tag{3.15}$$

For the second term, by substituting the solution (3.12) of the DI field, we obtain

(Second term in r.h.s. of (3.14))

$$= 4 \sum_j \sum_k \int_{t_0}^{t} \mathrm{d}t''\, C_{ijk}\, C_{knj}\, \overline{G^{(0)}_{kk/jkn}(t|t'')\, X^{(0)}_{n/jkn}(t'')\, X^{(0)}_{n/jkn}(t')\, X^{(0)}_{j/jkn}(t)\, X^{(0)}_{j/jkn}(t'')}$$

$$= 4 \sum_j \sum_k \int_{t_0}^{t} \mathrm{d}t''\, C_{ijk}\, C_{knj}\, \overline{G_{kk}(t|t'')}\, V_{nn}(\max\{t',t''\},\min\{t',t''\})\, V_{jj}(t,t'') \ , \tag{3.16}$$

where use has been made of DIA assumptions 1 and 2. The independency between $G^{(0)}_{in/ijk}$ and $X^{(0)}_{j/ijk}$ follows from the assumption that $X^{(0)}_{j/ijk} \approx X_j$ and DIA assumption 2(II). The third term is similarly calculated to be

(Third term in r.h.s. of (3.14))

$$= 2 \sum_j \sum_k \int_{t_0}^{t'} \mathrm{d}t''\, C_{ijk}\, C_{njk}\, \overline{G_{nn}(t'|t'')}\, V_{jj}(t,t'')\, V_{kk}(t,t'') \ , \tag{3.17}$$

by the use of (3.12). Thus the equation for the correlation function is written in terms of the correlation function itself and the response function $\overline{G}_{in}$ as

$$\left[\frac{\partial}{\partial t} + \nu\right] V_{in}(t,t') = 4 \sum_j \sum_k \int_{t_0}^{t} \mathrm{d}t''\, C_{ijk}\, C_{knj}\, \overline{G_{kk}(t|t'')}\, V_{nn}(\max\{t',t''\},\min\{t',t''\})\, V_{jj}(t,t'')$$
$$+ 2 \sum_j \sum_k \int_{t_0}^{t'} \mathrm{d}t''\, C_{ijk}\, C_{njk}\, \overline{G_{nn}(t'|t'')}\, V_{jj}(t,t'')\, V_{kk}(t,t'') \qquad (t > t') \ . \tag{3.18}$$

For the one-time correlation function, the forcing term in (2.10) is rewritten as

$$\overline{F_i(t)\, X_n(t)} = \tfrac{1}{2}\, \Delta t\, \sigma^2\, \delta_{in} = \frac{\nu}{N}\, \delta_{in} \ , \tag{3.19}$$

and the nonlinear terms are calculated in a manner similar to the above. Then, we obtain

$$\left[\frac{\mathrm{d}}{\mathrm{d}t} + 2\nu\right] V_{in}(t,t) = 4 \sum_j \sum_k \int_{t_0}^{t} \mathrm{d}t'\, C_{ijk}\, C_{knj}\, \overline{G_{kk}(t|t')}\, V_{nn}(t,t')\, V_{jj}(t,t')$$
$$+ 2 \sum_j \sum_k \int_{t_0}^{t} \mathrm{d}t'\, C_{ijk}\, C_{njk}\, \overline{G_{nn}(t|t')}\, V_{jj}(t,t')\, V_{kk}(t,t')$$
$$+ \frac{\nu}{N}\, \delta_{in} + (i \leftrightarrow n) \ . \tag{3.20}$$

3.3 Response function

An ensemble average of (3.2) for the response function is written as

$$\left[\frac{\partial}{\partial t} + \nu\right] \overline{G_{in}(t|t')} = \sum_j \sum_k 2\, C_{ijk} \overline{X_j(t)\, G_{kn}(t|t')} \ . \tag{3.21}$$

The right-hand side of this equation may be calculated in the same way as in the proceeding subsection. Substitution of direct-interaction decomposition (3.8) into the right-hand side leads to

$$\sum_j \sum_k 2\, C_{ijk} \overline{X_j(t)\, G_{kn}(t|t')} = \sum_j \sum_k 2\, C_{ijk} \overline{X_j(t)\, G^{(0)}_{kn/jkn}(t|t')}$$
$$+ \sum_j \sum_k 2\, C_{ijk} \overline{X_j(t)\, G^{(1)}_{kn/jkn}(t|t')} \ . \tag{3.22}$$

Thanks to DIA assumption 2(II), the first term in the right-hand side of (3.22) vanishes. By substituting expression (3.13) of the DI field $G^{(1)}_{kn}$ and decomposition (3.4), we rewrite the second term as

$$\text{(Second term in r.h.s. of (3.22))} = 4 \sum_j \sum_k \int_{t'}^{t} \mathrm{d}t''\ C_{ijk}\, C_{knj}\, V_{jj}(t,t'')\, \overline{G_{kk}(t|t'')}\, \overline{G_{nn}(t''|t')}\ , \quad (3.23)$$

where use has been made of DIA assumptions 1 and 2 and the assumption that $\overline{G^{(0)}_{ij/ijk}} = 0$. This last assumption follows from DIA assumption 2(I) and the approximation[3] $G^{(0)}_{ij/i_0j_0k_0} \approx \delta X^{(0)}_{i/i_0j_0k_0} / \delta X^{(0)}_{j/i_0j_0k_0}$. The influence of $X^{(0)}_{i/ijk}(t')$ on $X^{(0)}_{j/ijk}(t)$ $(t > t')$ should be very small because there is no direct interaction between these modes. Thus, the temporal evolution of the response function is described by

$$\left[\frac{\partial}{\partial t} + \nu \right] \overline{G_{in}(t|t')} = 4 \sum_j \sum_k \int_{t'}^{t} \mathrm{d}t''\ C_{ijk}\, C_{knj}\, V_{jj}(t,t'')\, \overline{G_{kk}(t|t'')}\, \overline{G_{nn}(t''|t')}\ . \quad (3.24)$$

In summary, (3.18), (3.20) and (3.24) construct a closed set of equations for the correlation and the response functions. A closed system for the auto-correlation function V_{ii} and the auto-response function $\overline{G}_{ii}$ follows by putting $i = n$ in these equations.

4 Reynolds-number reversed expansion

In this section we consider model equation (2.1) in the limit of weak nonlinearity. We start with linear equation and treat the nonlinear term as a perturbation. To make the formulation clearer, we introduce

$$\lambda = \frac{1}{\nu}\ , \quad (4.1)$$

which represents the ratio of the nonlinear to the viscous terms and will be called the Reynolds number on the analogy with the Navier-Stokes equation. Introducing a rescaled time

$$\tilde{t} = \nu\, t\ , \quad (4.2)$$

we rewrite (2.1), (3.1)—(3.3) respectively as

$$\frac{\mathrm{d}}{\mathrm{d}\tilde{t}} \tilde{X}_i(\tilde{t}) = \lambda \sum_j \sum_k C_{ijk}\, \tilde{X}_j(\tilde{t})\, \tilde{X}_k(\tilde{t}) - \tilde{X}_i(\tilde{t}) + \tilde{F}_i(\tilde{t})\ , \quad (4.3)$$

$$\tilde{G}_{in}(\tilde{t}|\tilde{t}') = \frac{\delta \tilde{X}_i(\tilde{t})}{\delta \tilde{X}_n(\tilde{t}')} \qquad (\tilde{t} \geq \tilde{t}')\ , \quad (4.4)$$

$$\frac{\partial}{\partial \tilde{t}} \tilde{G}_{in}(\tilde{t}|\tilde{t}') = \lambda \sum_j \sum_k 2\, C_{ijk}\, \tilde{X}_j(\tilde{t})\, \tilde{G}_{kn}(\tilde{t}|\tilde{t}') - \tilde{G}_{in}(\tilde{t}|\tilde{t}') \qquad (\tilde{t} > \tilde{t}') \quad (4.5)$$

[3]The evolution equation for $\widehat{G}^{(0)}_{ij/i_0j_0k_0} = \delta X^{(0)}_{i/i_0j_0k_0} / \delta X^{(0)}_{j/i_0j_0k_0}$ is derived from (2.1) as

$$\frac{\partial}{\partial t} \widehat{G}^{(0)}_{in/i_0j_0k_0}(t|t') = \sum_j \sum_k{}' 2\, C_{ijk}\, X^{(0)}_{j/i_0j_0k_0}(t)\, \widehat{G}^{(0)}_{kn/i_0j_0k_0}(t|t') - \nu\, \widehat{G}^{(0)}_{in/i_0j_0k_0}(t|t')\ .$$

$\sum'$: $\{i,j,k\} \neq \{i_0,j_0,k_0\}$

A comparison between this equation and (3.9) may justify that $|\widehat{G}^{(0)}_{ij} - G^{(0)}_{ij}| \ll |G^{(0)}_{ij}|$ because $X_j(t) \approx X^{(0)}_{j/i_0j_0k_0}$.

and

$$\widetilde{G}_{in}(\widetilde{t}|\widetilde{t}) = \delta_{in} \ , \tag{4.6}$$

where $\widetilde{X}_i(\widetilde{t}) = X_i(t)$ and $\widetilde{F}_i(\widetilde{t}) = F_i(t)/\nu$. For simplicity of notations, we omit the tildes on $\widetilde{t}$, $\widetilde{X}_i$, $\widetilde{G}_{in}$ and $\widetilde{F}_i$ in §§4.1—4.3.

4.1 Reynolds-number expansion

For small Reynolds numbers $\lambda \ll 1$ (i.e., $\nu \gg 1$) it may be legitimate to expand X_i and G_{in} in power series of λ as

$$X_i(t) = X_i^{(0)}(t) + \lambda\, X_i^{(1)}(t) + O(\lambda^2) \tag{4.7}$$

$$G_{in}(t|t') = G_{in}^{(0)}(t|t') + \lambda\, G_{in}^{(1)}(t|t') + O(\lambda^2) \ . \tag{4.8}$$

By substituting these equations into (4.3) and (4.5), we obtain, at $O(1)$,

$$\frac{\mathrm{d}}{\mathrm{d}t}\, X_i^{(0)}(t) = -X_i^{(0)}(t) + F_i(t) \tag{4.9}$$

and

$$\frac{\partial}{\partial t}\, G_{in}^{(0)}(t|t') = -G_{in}^{(0)}(t|t') \ , \tag{4.10}$$

while, at $O(\lambda)$,

$$\frac{\mathrm{d}}{\mathrm{d}t}\, X_i^{(1)}(t) = \sum_j \sum_k C_{ijk}\, X_j^{(0)}(t)\, X_k^{(0)}(t) - X_i^{(1)}(t) \tag{4.11}$$

and

$$\frac{\partial}{\partial t}\, G_{in}^{(1)}(t|t') = \sum_j \sum_k 2\, C_{ijk}\, X_j^{(0)}(t)\, G_{kn}^{(0)}(t|t') - G_{in}^{(1)}(t|t') \ . \tag{4.12}$$

The boundary conditions of response functions $G_{in}^{(0)}$ and $G_{in}^{(1)}$ are respectively written, from (4.6), as

$$G_{in}^{(0)}(t|t) = \delta_{in} \tag{4.13}$$

and

$$G_{in}^{(1)}(t|t) = 0 \ . \tag{4.14}$$

It follows from (4.10), (4.11) and (4.13) that

$$X_i^{(1)}(t) = \sum_a \sum_b \sum_c \int_{t_0}^{t} \mathrm{d}t'' C_{abc}\, G_{ia}^{(0)}(t|t'')\, X_b^{(0)}(t'')\, X_c^{(0)}(t'') \ , \tag{4.15}$$

and from (4.10) and (4.12)—(4.14) that

$$G_{in}^{(1)}(t|t') = \sum_a \sum_b \sum_c \int_{t'}^{t} \mathrm{d}t''\, 2\, C_{abc}\, G_{ia}^{(0)}(t|t'')\, X_b^{(0)}(t'')\, G_{cn}^{(0)}(t''|t') \ . \tag{4.16}$$

Here, we have assumed that

$$X_i^{(1)}(t_0) = 0 \ . \tag{4.17}$$

4.2 Correlation function

The evolution equations for the correlation function (2.8) are derived from (4.3) as

$$\left[\frac{\partial}{\partial t}+1\right] V_{in}(t,t') = \lambda \sum_j \sum_k C_{ijk}\, \overline{X_j(t)\, X_k(t)\, X_n(t')} \qquad (t>t') \tag{4.18}$$

and

$$\left[\frac{\mathrm{d}}{\mathrm{d}t}+2\right] V_{in}(t,t) = \lambda \sum_j \sum_k C_{ijk}\, \overline{X_j(t)\, X_k(t)\, X_n(t)} + \frac{1}{N}\,\delta_{in} + (i \leftrightarrow n)\ . \tag{4.19}$$

Substitution of the Reynolds-number expansion (4.7) and (4.8) into the right-hand side of (4.18) leads to

$$\begin{aligned}\lambda \sum_j \sum_k C_{ijk}\, \overline{X_j(t)\, X_k(t)\, X_n(t')} &= \lambda \sum_j \sum_k C_{ijk}\, \overline{X_j^{(0)}(t)\, X_k^{(0)}(t)\, X_n^{(0)}(t')} \\ &+ \lambda^2 \sum_j \sum_k 2\, C_{ijk}\, \overline{X_j^{(0)}(t)\, X_k^{(1)}(t)\, X_n^{(0)}(t')} \\ &+ \lambda^2 \sum_j \sum_k C_{ijk}\, \overline{X_j^{(0)}(t)\, X_k^{(0)}(t)\, X_n^{(1)}(t')}\ ,\end{aligned} \tag{4.20}$$

where the terms of $O(\lambda^3)$ are neglected under the assumption of small Reynolds number. Since $X_i^{(0)}$ is a solution of the linear equation (4.9) excited by a Gaussian random force, it obeys a joint normal probability distribution with vanishing covariance. This leads to

$$\text{(First term in r.h.s. of (4.20))} = 0\ . \tag{4.21}$$

The second term of (4.20) can be written, on substitution of the solution (4.15) of $X_i^{(1)}$, as

$$\begin{aligned}&\text{(Second term in r.h.s. of (4.20))} \\ &= 2\lambda^2 \sum_j \sum_k \sum_a \sum_b \sum_c \int_{t_0}^{t} \mathrm{d}t''\, C_{abc}\, C_{ijk}\, \overline{G_{ka}^{(0)}(t|t'')\, X_j^{(0)}(t)\, X_n^{(0)}(t')\, X_b^{(0)}(t'')\, X_c^{(0)}(t'')} \\ &= 2\lambda^2 \sum_j \sum_k \sum_a \sum_b \sum_c \int_{t_0}^{t} \mathrm{d}t''\, C_{abc}\, C_{ijk}\, \overline{G_{ka}^{(0)}(t|t'')} \Big[\, \overline{X_j^{(0)}(t)\, X_n^{(0)}(t')}\ \overline{X_b^{(0)}(t'')\, X_c^{(0)}(t'')} \\ &\qquad + \overline{X_j^{(0)}(t)\, X_b^{(0)}(t'')}\ \overline{X_n^{(0)}(t')\, X_c^{(0)}(t'')} \\ &\qquad + \overline{X_j^{(0)}(t)\, X_c^{(0)}(t'')}\ \overline{X_n^{(0)}(t')\, X_b^{(0)}(t'')}\, \Big] \\ &= 4\lambda^2 \sum_j \sum_k \int_{t_0}^{t} \mathrm{d}t''\, C_{knj}\, C_{ijk}\, \overline{G_{kk}^{(0)}(t|t'')}\ \overline{X_j^{(0)}(t)\, X_j^{(0)}(t'')}\ \overline{X_n^{(0)}(t')\, X_n^{(0)}(t'')}\ .\end{aligned} \tag{4.22}$$

Here, we have used the relation

$$G_{in}^{(0)}(t|t') = \delta_{in}\, G_{ii}^{(0)}(t|t') \tag{4.23}$$

and the assumption of independency between $X_i^{(0)}$ and $G_{in}^{(0)}$, both of which may be justified by the fact that $G_{in}^{(0)}$ is a solution of the linear equation (4.10) with the initial condition (4.13).

Now, we employ the procedure of so-called reversion to rewrite (4.22). Substitution of the Reynolds-number expansion (4.7) into the definition (2.8) of the correlation function gives

$$V_{in}(t,t') = V_{in}^{(0)}(t,t') + \lambda \left[\overline{X_i^{(0)}(t)\, X_n^{(1)}(t')} + \overline{X_i^{(1)}(t)\, X_n^{(0)}(t')} \right] + O(\lambda^2)$$
$$= V_{in}^{(0)}(t,t') + O(\lambda) \,, \tag{4.24}$$

where $V_{in}^{(0)}$ is defined by

$$V_{in}^{(0)}(t,t') = \overline{X_i^{(0)}(t)\, X_n^{(0)}(t')} \,. \tag{4.25}$$

For the response function, the ensemble average of (4.8) yields

$$\overline{G_{in}(t|t')} = \overline{G_{in}^{(0)}(t|t')} + O(\lambda) \,. \tag{4.26}$$

The $O(\lambda)$ and the higher-order terms in (4.24) and (4.26) can be expressed in terms of $\boldsymbol{V}^{(0)}$ and $\overline{\boldsymbol{G}^{(0)}}$ in principle (e.g. (4.15) and (4.16) for the $O(\lambda)$ terms). We can then regard (4.24) and (4.26) as the equations for $V_{in}^{(0)}$ and $\overline{G_{in}^{(0)}}$, the solution of which is written in power series of λ as

$$V_{in}^{(0)}(t,t') = V_{in}(t,t') + O(\lambda) \tag{4.27}$$

$$\overline{G_{in}^{(0)}(t|t')} = \overline{G_{in}(t|t')} + O(\lambda) \,. \tag{4.28}$$

This procedure is called the reversion [8], which the naming of the Reynolds-number reversed expansion (RRE) originates from. Equation (4.22) is then written in terms of the true field variables $\boldsymbol{V}$ and $\overline{\boldsymbol{G}}$ as

$$(4.22) = 4\lambda^2 \sum_j \sum_k \int_{t_0}^{t} \mathrm{d}t''\, C_{knj}\, C_{ijk}\, \overline{G_{kk}(t|t'')}\; V_{jj}(t,t'')\, V_{nn}(\max\{t',t''\}, \min\{t',t''\}) \tag{4.29}$$

at the leading order. The third term of (4.20) can be estimated in a similar manner as

$$\text{(Third term in r.h.s. of (4.20))}$$
$$= 2\lambda^2 \sum_j \sum_k \int_{t_0}^{t'} \mathrm{d}t''\, C_{njk}\, C_{ijk}\, \overline{G_{nn}(t'|t'')}\; V_{jj}(t,t'')\, V_{kk}(t,t'') \,. \tag{4.30}$$

Thus, combination of (4.20), (4.21), (4.29) and (4.30) finally reduces the evolution equation for the two-time correlation function into

$$\left[\frac{\partial}{\partial t} + 1 \right] V_{in}(t,t') = 4\lambda^2 \sum_j \sum_k \int_{t_0}^{t} \mathrm{d}t''\, C_{knj}\, C_{ijk}\, \overline{G_{kk}(t|t'')}\; V_{jj}(t,t'')\, V_{nn}(\max\{t',t''\}, \min\{t',t''\})$$
$$+ 2\lambda^2 \sum_j \sum_k \int_{t_0}^{t'} \mathrm{d}t''\, C_{njk}\, C_{ijk}\, \overline{G_{nn}(t'|t'')}\; V_{jj}(t,t'')\, V_{kk}(t,t'') \,. \tag{4.31}$$

Equation (4.19) for the one-time correlation function is similarly derived as

$$\left[\frac{\mathrm{d}}{\mathrm{d}t} + 2 \right] V_{in}(t,t) = 4\lambda^2 \sum_j \sum_k \int_{t_0}^{t} \mathrm{d}t'\, C_{knj}\, C_{ijk}\, \overline{G_{kk}(t|t')}\; V_{jj}(t,t')\, V_{nn}(t,t')$$
$$+ 2\lambda^2 \sum_j \sum_k \int_{t_0}^{t} \mathrm{d}t'\, C_{njk}\, C_{ijk}\, \overline{G_{nn}(t|t')}\; V_{jj}(t,t')\, V_{kk}(t,t')$$
$$+ \frac{1}{N}\, \delta_{in} + (i \leftrightarrow n) \,. \tag{4.32}$$

4.3 Response function

The evolution equation for the ensemble average of the response function is

$$\left[\frac{\partial}{\partial t}+1\right]\overline{G_{in}(t|t')}=\lambda\sum_j\sum_k 2C_{ijk}\,\overline{X_j(t)\,G_{kn}(t|t')}\,, \tag{4.33}$$

which follows from (4.5). Substituting (4.7) and (4.8) into the right-hand side of this equation and discarding the terms of $O(\lambda^3)$, we obtain

$$\begin{aligned}\lambda\sum_j\sum_k 2C_{ijk}\,\overline{X_j(t)\,G_{kn}(t|t')}=\lambda\sum_j\sum_k 2C_{ijk}\,\overline{X_j^{(0)}(t)\,G_{kn}^{(0)}(t|t')}\\ +\lambda^2\sum_j\sum_k 2C_{ijk}\,\overline{X_j^{(1)}(t)\,G_{kn}^{(0)}(t|t')}\\ +\lambda^2\sum_j\sum_k 2C_{ijk}\,\overline{X_j^{(0)}(t)\,G_{kn}^{(1)}(t|t')}\,.\end{aligned} \tag{4.34}$$

In the same way as in the preceding subsection we can write each term in this equation in terms of $\boldsymbol{V}$ and $\overline{\boldsymbol{G}}$. Then, (4.34) is converted into

$$\left[\frac{\partial}{\partial t}+1\right]\overline{G_{in}(t|t')}=4\lambda^2\sum_j\sum_k\int_{t'}^{t}\mathrm{d}t''\,C_{ijk}\,C_{knj}\,V_{jj}(t,t'')\,\overline{G_{kk}(t|t'')}\;\overline{G_{nn}(t''|t')}\,. \tag{4.35}$$

4.4 Comparison of two approximations

In the formulation made in the last three subsections the time was scaled as $\widetilde{t}=\nu t=t/\lambda$ (see (4.1) and (4.2), and remember the omission of the tilde). If $\widetilde{t}$ is transformed back to t in the resultant equations (4.31), (4.32) and (4.35), they become identical to (3.18), (3.20) and (3.24), respectively, which are derived by DIA. Incidentally a so-called bookkeeping parameter ($\lambda=1$), which is sometimes introduced in this kind of expansion [3,7,11], plays a role similar to the time transformation such as (4.2).

The RRE described in the preceding subsections is based upon an idea developed by Kraichnan [8]. He showed it for the Navier-Stokes equation that those integro-differential equations derived by DIA (both in the Eulerian and the Lagrangian formulations) are also obtained by the use of RRE. Kaneda [3] applied this expansion (called the Lagrangian renormalized approximation by him) to the Lagrangian velocity field. The resulting integro-differential equations are again the same as those derived by DIA [4].

Now we know that the above two approximations lead to a same set of equations in each case of model equation (2.1) and the Navier-Stokes equation. The discussion on the differences between these approximations for the model equation, which will be made in the next section, is therefore expected to be applied to the Navier-Stokes equation as well.

5 Applicability of DIA

5.1 Solution to DIA equations

In previous sections we have shown that an identical system of equations is derived by two completely different approximations. It is quite obvious that RRE should be valid for small Reynolds numbers ($\nu \gg 1$), whereas the assumptions of DIA summarized in §3.1 be for the large degrees of freedom ($N \gg 1$). We expect, therefore, that the equations (hereafter, called the DIA *equations*) may give good predictions in such parameter ranges that $\nu \gg 1$ or $N \gg 1$. This expectation will be verified in the following by a series of direct numerical simulations of the model equation.

By construction (see (2.7)), the coefficients C_{ijk} do not depend on the absolute value of the suffixes but only on their difference, and therefore the system can be statistically homogeneous (e.g., $\dot{V}_{ii}$ can be independent of i). If the system is statistically stationary as well as homogeneous, the auto-correlation and the response functions are expressed as

$$V_{ii}(t,t') = \mathcal{V}(t-t') \ , \tag{5.1}$$

$$\overline{G_{ii}(t,t')} = \mathcal{G}(t-t') \ . \tag{5.2}$$

Then, the DIA equations (3.18), (3.20) and (3.24) for $i = n$ are respectively written as

$$\left[\frac{\mathrm{d}}{\mathrm{d}\tau} + \nu\right] \mathcal{V}(\tau) = -2c_1 \int_0^\infty \mathrm{d}\tau' \, \mathcal{G}(\tau') \, \mathcal{V}(|\tau - \tau'|) \, \mathcal{V}(\tau') + 2c_1 \int_\tau^\infty \mathrm{d}\tau' \, \mathcal{G}(\tau' - \tau) \, \mathcal{V}(\tau') \, \mathcal{V}(\tau') \qquad (\tau > 0) \ , \tag{5.3}$$

$$\mathcal{V}(0) = \frac{1}{N} \tag{5.4}$$

and

$$\left[\frac{\mathrm{d}}{\mathrm{d}\tau} + \nu\right] \mathcal{G}(\tau) = -2c_1 \int_0^\tau \mathrm{d}\tau' \ \mathcal{V}(\tau') \, \mathcal{G}(\tau') \, \mathcal{G}(\tau - \tau') \ , \tag{5.5}$$

with boundary condition

$$\mathcal{G}(0) = 1 \tag{5.6}$$

(see (3.3)). Here, the coefficient c_1 is defined by [4]

$$c_1 = \sum_j \sum_k C_{ijk} \, C_{ijk} \ . \tag{5.7}$$

[4] Notice the relation

$$c_2 = \sum_j \sum_k C_{ijk} \, C_{kij} = \sum_j \sum_k C_{ijk} \, (-C_{ijk} - C_{jki}) = \sum_j \sum_k C_{ijk} \, (-C_{ikj} - C_{jik}) = -c_1 - c_2 \ ,$$

which implies that $c_2 = -\frac{1}{2} c_1$, where use has been made of (2.2) and (2.3).

Notice here that the original upper bound $t - t_0$ of integrations in (5.3) has been replaced by the infinity. This will be justified *a posteriori* by taking it to be sufficiently larger than the decaying time-scale of $\mathcal{V}(\tau)$ and $\mathcal{G}(\tau)$ (see §5.2).

Equations (5.3)—(5.6) permit a solution such that

$$\mathcal{V}(\tau) = \mathcal{V}(0)\,\mathcal{G}(\tau) \tag{5.8}$$

and

$$\left[\frac{\mathrm{d}}{\mathrm{d}\tau} + \nu\right] \mathcal{G}(\tau) = -2c_1\,\mathcal{V}(0) \int_0^\tau \mathrm{d}\tau' \,\left[\mathcal{G}(\tau')\right]^2 \mathcal{G}(\tau - \tau') \,. \tag{5.9}$$

Incidentally, this equation shows that the decaying time-scale of $\mathcal{G}(\tau)$ (and $\mathcal{V}(\tau)$) is inversely proportional to $\sqrt{c_1\,\mathcal{V}(0)} = \sqrt{c_1/N}$ in the inviscid limit (see Fig.3(b)).

Equation (5.9) with boundary condition (5.6) is solved numerically by an iteration method. The correlation function thus obtained are drawn in Figs.4 for various values of N and ν together with the results by the direct numerical simulation. A case of small number of degrees of freedom is shown in Figs.4(a)—(c) for three different values of viscosity $\nu = 10$, 1 and 0. It is seen that the agreement between the prediction by the DIA equation and the direct numerical simulation is better for larger values of ν. The agreement seems perfect even at $\nu = 1$ (see Fig.4(b)). We also compare them with a purely linear solution $\mathcal{V}(\tau) = \mathcal{V}(0)\,\exp[\,-\nu\tau\,]$ (shown with a dotted line). As seen in Fig.4(a), the three curves completely coincide with each other at $\nu = 10$, which means that the nonlinear effects may be negligible at this value of viscosity. It is interesting however to see in Fig.4(b) that the purely linear solution deviates substantially from the results of both the DIA equation and the direct numerical simulation. This indicates that the nonlinear effects on the correlation function, even though they are not so large, are properly evaluated by the DIA equations. In Figs.4(c)—(f), we compare the results of various values of N for vanishing viscosity (in the limit of large Reynolds number). It is seen that the agreement of the two improves as N increases. In conclusion, the prediction by the DIA equation works well for small Reynolds numbers ($\nu \gg 1$) or for large degrees of freedom ($N \gg 1$).

5.2 Validity of DIA assumptions

It was shown in the preceding subsection that the DIA equations give an excellent predictions of the auto-correlation function in the case of $N \gg 1$ or $\nu \gg 1$. This is quite reasonable because DIA and RRE are formulated for $N \gg 1$ and $\nu \gg 1$, respectively. Here we demonstrate it numerically that the assumptions of DIA summarized in §3.1 are actually satisfied for $N \gg 1$.

First, in order to examine DIA assumption 1 that the DI field is much smaller in magnitude than the NDI field during the decaying time-scale of the auto-correlation function, we compare, in Fig.5, the temporal evolution

of the magnitude of the DI field

$$D(t) = \left\langle \sum_i \left[X^{(1)}_{i/i_0 j_0 k_0}(t|0) \right]^2 \right\rangle \tag{5.10}$$

for four different values of N in the inviscid case. Here $\langle \quad \rangle$ stands for an average over a sufficiently large number of runs starting with random initial conditions. The time in the horizontal axis is normalized by the decaying time-scale of the auto-correlation function (cf. Fig.3(b)). Indeed the DI field develops in time, but it never exceeds the NDI field in magnitude within the correlation time, namely, $D(t) < \sum_i \left[X^{(0)}_i\right]^2 = 1$ for $\sqrt{c_1/N}\, t < 2$. Moreover, $D(t)$ decreases roughly in the inverse proportion to N. This concludes that DIA assumption 1 may be better for larger values of N.

A remark on the replacement of the upper bound of the integrations in (5.3) may be in order. Remember that the DIA equations are formulated under the assumption that the DI fields are smaller in magnitude than the NDI fields. The behavior of $D(t)$ shown in Fig.5 tells us that when we choose the direct-interaction decomposition time t_0 so that $t - t_0$ may be sufficiently larger than the correlation time, DIA assumption 1 is actually satisfied if $N \gg 1$. Then, thanks to the exponential decay of $\mathcal{G}(\tau)$ and $\mathcal{V}(\tau)$, we can replace $t - t_0$ by the infinity.

Next, we move to DIA assumption 2(I) on the independency among the modes without direct interactions. This assumption is used in the derivation of the DIA equations as

$$\overline{X^{(0)}_{i/ijk}(t)\, X^{(0)}_{j/ijk}(t)\, X^{(0)}_{k/ijk}(t')} = 0 \tag{5.11}$$

(see (3.15)). In order to assess this assumption quantitatively, we calculate the triple correlation factor

$$R_{ijk}(t-t') = \frac{\overline{X_i(t)\, X_j(t)\, X_k(t')}}{\sqrt{\overline{X_i(t)^2}\;\overline{X_j(t)^2}\;\overline{X_k(t)^2}}} \tag{5.12}$$

for the true field and for the NDI field (where $X_i(t)$ is replaced by $X^{(0)}_{i/ijk}$). In Figs.6, we plot the results for $\{i,j,k\} = \{1,2,4\}$ for (a) $N = 7$ and (b) 20 in the inviscid case. It is clear from Figs.6(b) that the triple correlation factor for the NDI field is drastically reduced for larger N. This gives a strong support of the validity of (5.11) for $N \gg 1$. As seen in Figs.6(a), on the other hand, it does not well behave for smaller N. This failure in the small-N case is due to the indirect interactions.

Finally, we consider DIA assumption 2(II) that $G^{(0)}_{in/ijk}$, $G^{(0)}_{jn/ijk}$ and X_k are statistically independent of each other. This is based on the fact that the governing equation (e.g. (3.9)) of each mode does not contain the other modes. This assumption is used, for example, as

$$\overline{G^{(0)}_{ij/ijk}(t|t')\, X_k(t)} = 0 \tag{5.13}$$

in the derivation of the DIA equations (see the paragraph below (3.22)). To check it we calculate a covariance factor

$$S_{ijk}(t-t') = \frac{\overline{G_{ij}(t|t')\, X_k(t)}}{\sqrt{\overline{X_k(t)^2}}} \tag{5.14}$$

for the true field and for the NDI field (where G_{ij} is replaced by $G^{(0)}_{ij/ijk}$). Notice that the assumption requires that this factor should vanish for the NDI field. In Figs.7, we plot the results of S_{412} for (a) $N = 7$ and (b) 20 in the inviscid case. The other factors such as S_{214} show similar behavior to S_{412} (figures are omitted). It is seen that S_{412} tends to vanish for larger N like R_{ijk} (see Figs.6). In conclusion, DIA assumption 2(II) is also satisfied for $N \gg 1$.

5.3 Strong nonlinear coupling

So far we have dealt with a system (2.1) with weak nonlinear coupling (see §2.1 for the definition) for which DIA works excellently. Now we examine what happens if there are many direct interactions. By removing the condition in (2.7), we define here the coefficient C_{ijk} by

$$C_{ijk} = \begin{cases} 0 & (\text{ if } i=j \text{ or } j=k \text{ or } k=i\ ) \quad (5.15a) \\ \frac{1}{3}N - b & (\text{ otherwise }) \ . \quad (5.15b) \end{cases}$$

Model equation (2.1) with coefficients (5.15) contains much more direct interactions between each pair of modes than that with weak coupling coefficients (2.6) and (2.7). Hence, even if only a single interaction is extracted, a substantial amount of correlation may remain. In order to check whether DIA assumption 2(I) is actually satisfied in this strong nonlinear coupling case, we calculate the triple correlation factor (5.12) for the true and the NDI fields. The results are shown in Figs.8 for (a) $N = 7$ and (b) 20 in the inviscid case. It is seen that the correlation factor for the NDI field is not smaller (on the contrary, it is even larger) than that for the true field both for small and large N. This indicates that DIA assumption 2(I) dose not hold in a system with strong nonlinear coupling.

The auto-correlation function, which is calculated in the same way as in §§2.2 and 5.1, is plotted in Figs.9 for various values of N and ν. Here, a thick line represents the prediction by the DIA equation, a thin line the numerical simulation result, and a broken line a linear solution. By comparing Figs.9(a)—(c), the agreement between the theory and the simulation becomes better and better as ν increases (or the Reynolds number decreases). On the other hand, as Figs.9(c) and (d) show, the agreement does not seem to improve for large N. Thus, it may be said that RRE works well at small Reynolds numbers for a system of strong nonlinear coupling, but DIA does not.

6 Concluding remarks

We have given a numerical evidence for a dynamical system that DIA and RRE have different parameter regions of validity though they lead to an identical set of equations for the correlation and the response functions. The RRE is applicable for the weak nonlinearity, whereas DIA is for the large degrees of freedom. We have also shown that DIA may work for a system with weak nonlinear coupling, whereas strength of the coupling does not matter for RRE.

In relation to the applications to the Navier-Stokes turbulence, it should be emphasized that the strength of the nonlinear coupling is important. We have seen that DIA works excellently for a system with weak nonlinear coupling but not for strong coupling. An important difference between these two cases is in the number of direct interactions. There is only a single, at the most, direct interaction between each pair of modes in the weak coupling, while plural numbers of interactions in the strong coupling. The Navier-Stokes equation for an incompressible fluid in a periodic box (of side L) is written as

$$\left[\frac{\partial}{\partial t}+\nu k^2\right]\widetilde{u}_i(\boldsymbol{k},t)=-\frac{\mathrm{i}}{2}\left(\frac{2\pi}{L}\right)^3\sum_{j=1}^{3}\sum_{m=1}^{3}\widetilde{P}_{ijm}(\boldsymbol{k})\sum_{(\boldsymbol{k}+\boldsymbol{p}+\boldsymbol{q}=o)}\sum_{\boldsymbol{q}}\widetilde{u}_j(-\boldsymbol{p},t)\,\widetilde{u}_m(-\boldsymbol{q},t)\;, \tag{6.1}$$

where ν, $\widetilde{P}_{ijm}(\boldsymbol{k})$ and $\widetilde{u}_i(\boldsymbol{k})$ denote the kinematic viscosity, a geometrical operator (due to the nonlinear and the pressure terms) and the Fourier component of the velocity for wavenumber $\boldsymbol{k}$ ($k=|\boldsymbol{k}|$), respectively (see [7] for example). There is a single direct interaction between each pair of $\widetilde{u}_i(\boldsymbol{k})$. Hence, an incompressible homogeneous isotropic turbulence is a system with *large* degrees of freedom and *strong* nonlinearity of *weak* coupling. This is the reason why DIA works well for the Navier-Stokes turbulence [4].

In this paper we have investigated the two extreme cases of nonlinear interactions, i.e., the weakest and the strongest couplings. The DIA does work in the former, but not in the latter. It is natural to ask what happens for a system with intermediate strength of nonlinear couplings. What determines the applicability of DIA? Is there a (system-size dependent) critical number of direct interactions? The type of the nonlinear interaction (other than the quadratic) may also be relevant. All of these interesting questions are left for a future study.

Acknowledgments

This work was partially supported by a Grant-in-Aid for Scientific Research from the Ministry of Education, Science and Culture.

References

[1] R. H. Kraichnan, J. Fluid Mech. **5** (1959) 497-543.

[2] R. H. Kraichnan, Phys. Fluids **8** (1965) 575-598. (erratum 1966, *ibid.*, 1884).

[3] Y. Kaneda, J. Fluid Mech. **107** (1981) 131-145.

[4] S. Kida & S. Goto, J. Fluid Mech. (1997) (in print).

[5] H. W. Wyld, Jr., Ann. Phys., N.Y. **14** (1961) 143-165.

[6] P. C. Martin, E. D. Siggia & H. A. Rose, Phys. Rev. A **8** (1973) 423-437.

[7] D. C. Leslie, *Developments in the theory of turbulence*. Clarendon Press (1973).

[8] R. H. Kraichnan, J. Fluid Mech. **83** (1977) 349-374.

[9] R. H. Kraichnan, J. Math. Phys. **2** (1961) 124-148.

[10] J. R. Herring & R. H. Kraichnan, in *Statistical models and turbulence*. (eds. M. Rosenblatt & C. Van Atta, Springer Verlog, 1972) 148-194.

[11] S. A. Orszag, in *Fluid Dynamics*. (eds. Balian, R. & Peube, J. L., Gordon & Breach, New York. 1977) 237-374.

[12] U. Frisch, M. Lesieur & A. Brissaud, J. Fluid Mech. **65** (1974) 145-152.

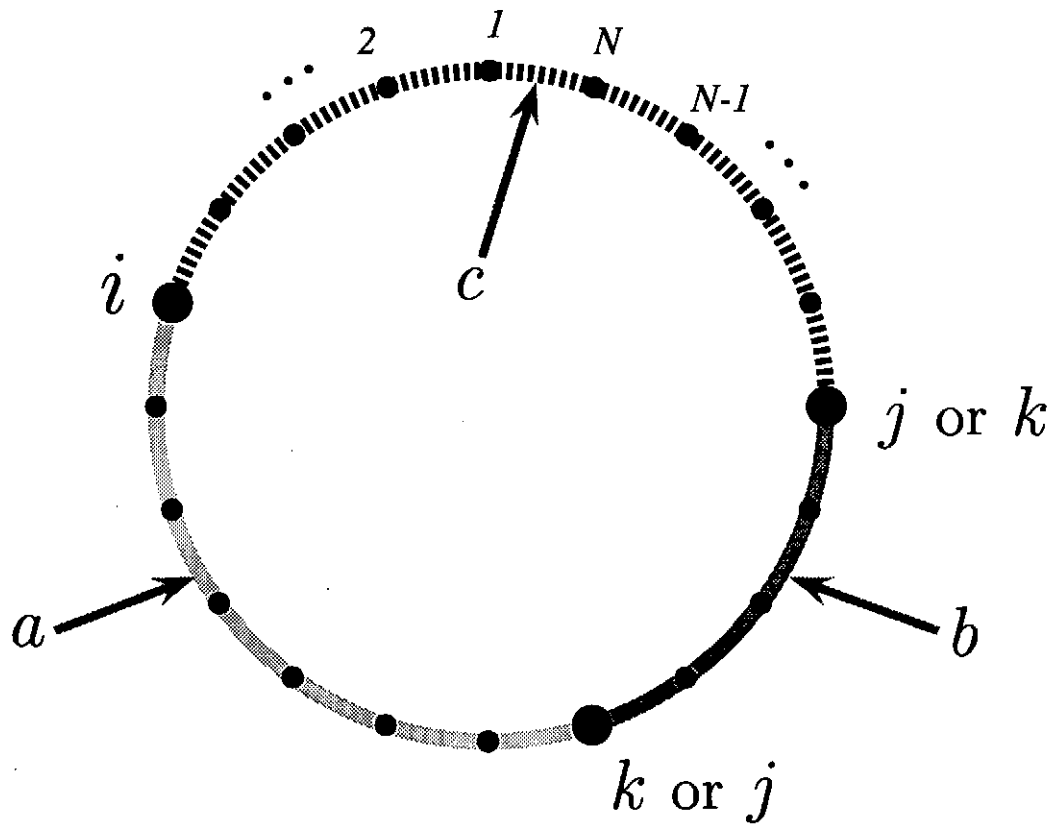

Fig.1 Definitions of a, b and c. N points are assigned with equal distance apart on a circle of circumference N. The arc lengths a, b and c between points i, j and k are defined in such a way that point i is located between a and c, and that a, b and c are placed counterclockwise.

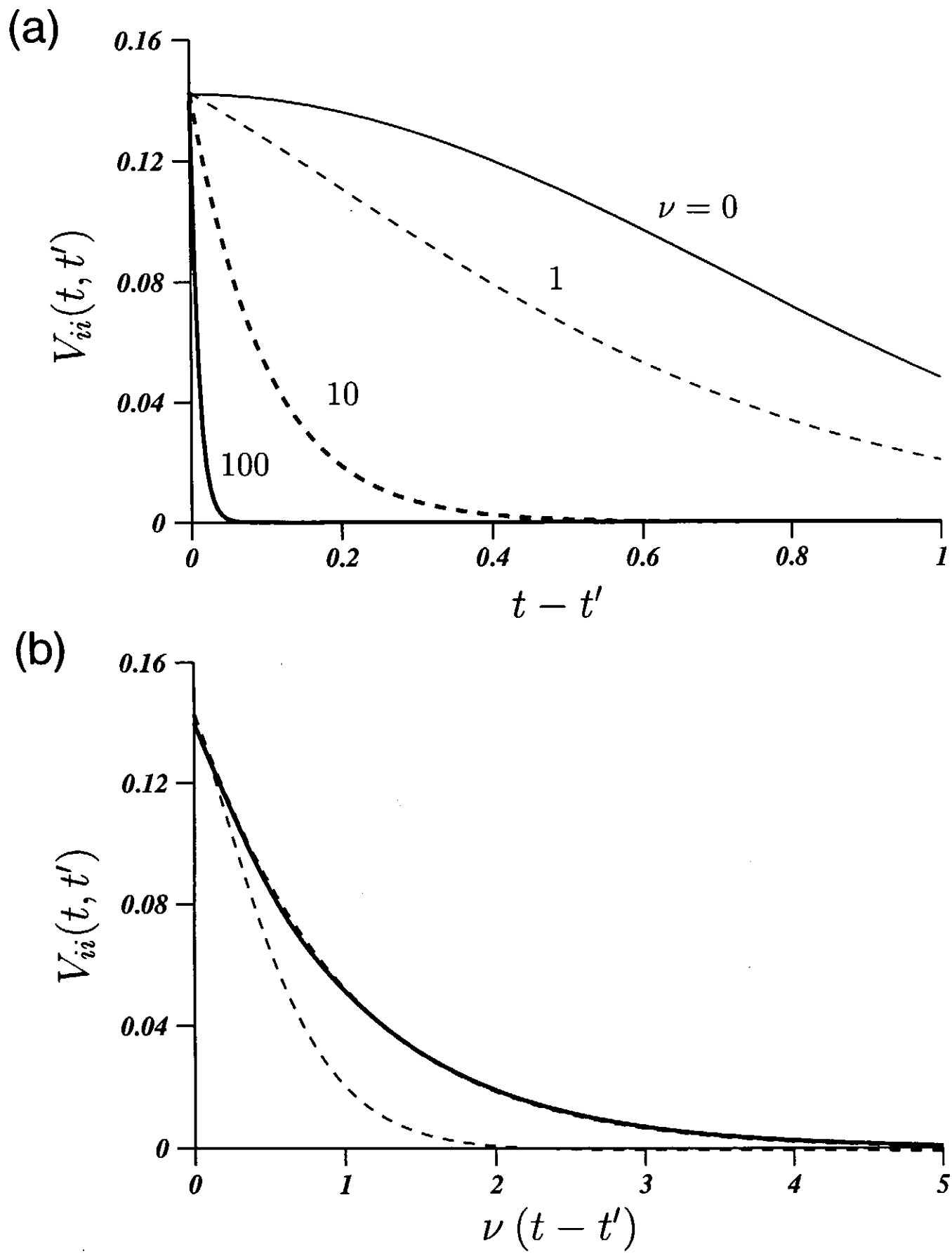

Fig.2 (a) Auto-correlation functions $V_{ii}(t,t') = \overline{X_i(t)X_i(t')}$ for $N = 7$ and $\nu = 0$ (thin solid line), 1 (thin broken line), 10 (thick broken line) and 100 (thick solid line). (b) Same as (a) but for a rescaled time.

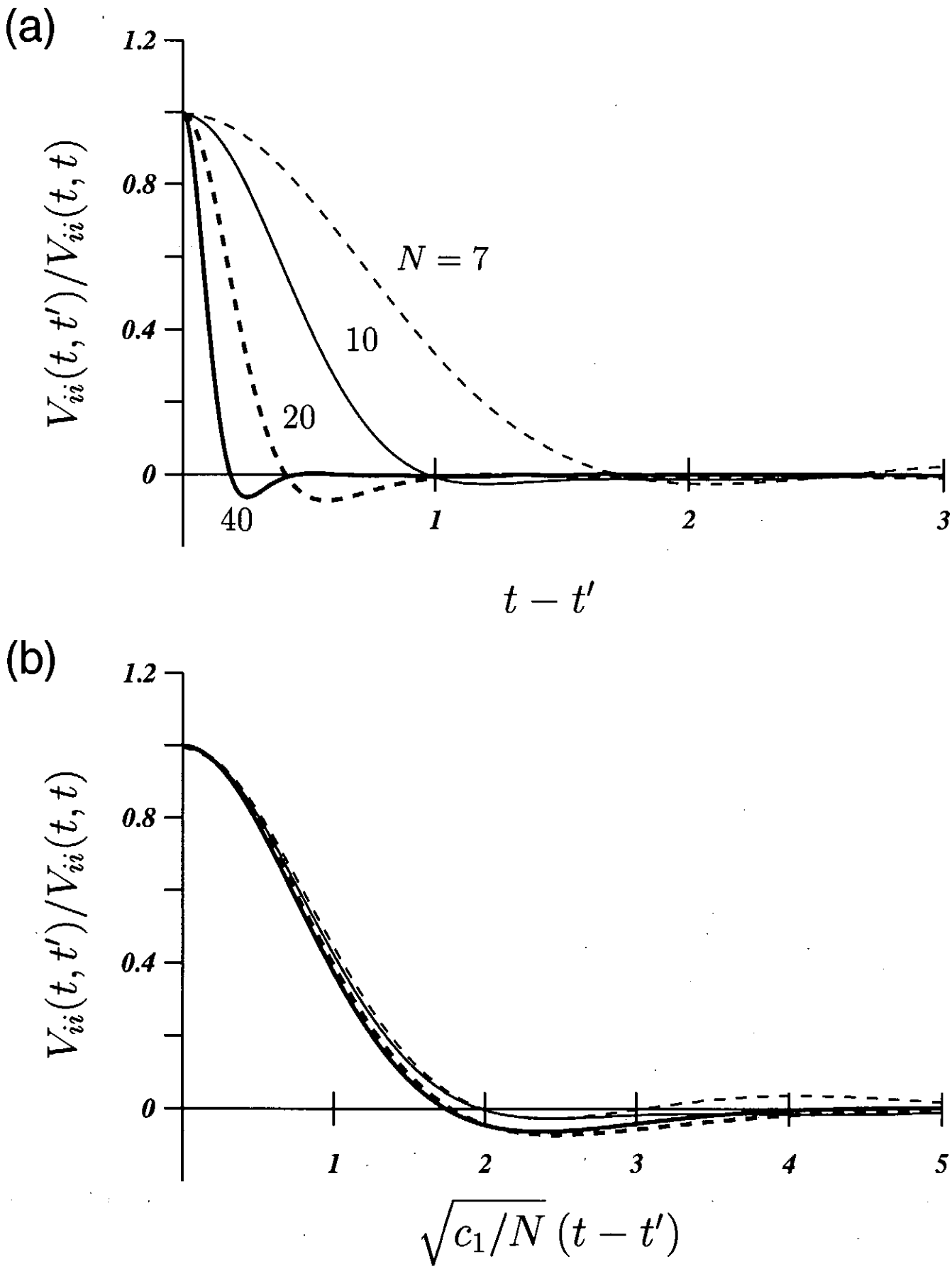

Fig.3 (a) Auto-correlation functions normalized by $V_{ii}(t,t)$ for $\nu = 0$. The degrees of freedom $N = 7$ (thin broken line), 10 (thin solid line), 20 (thick broken line) and 40 (thick solid line). (b) Same as (a) but for a rescaled time (see (5.7) for the definition of c_1).

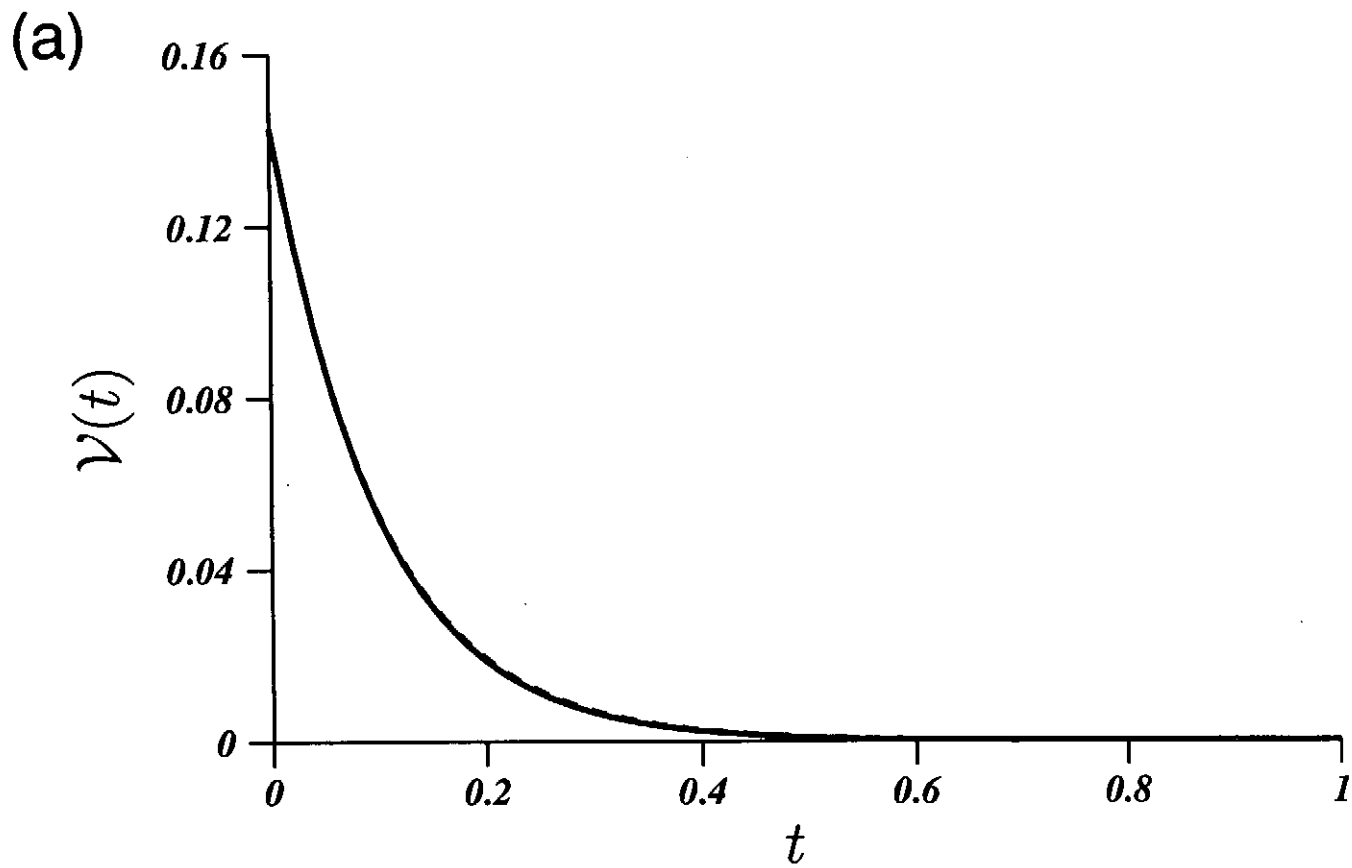
(a)
0.16
0.12
0.08
0.04
0
$\mathcal{V}(t)$
0
0.2
0.4
0.6
0.8
1
t

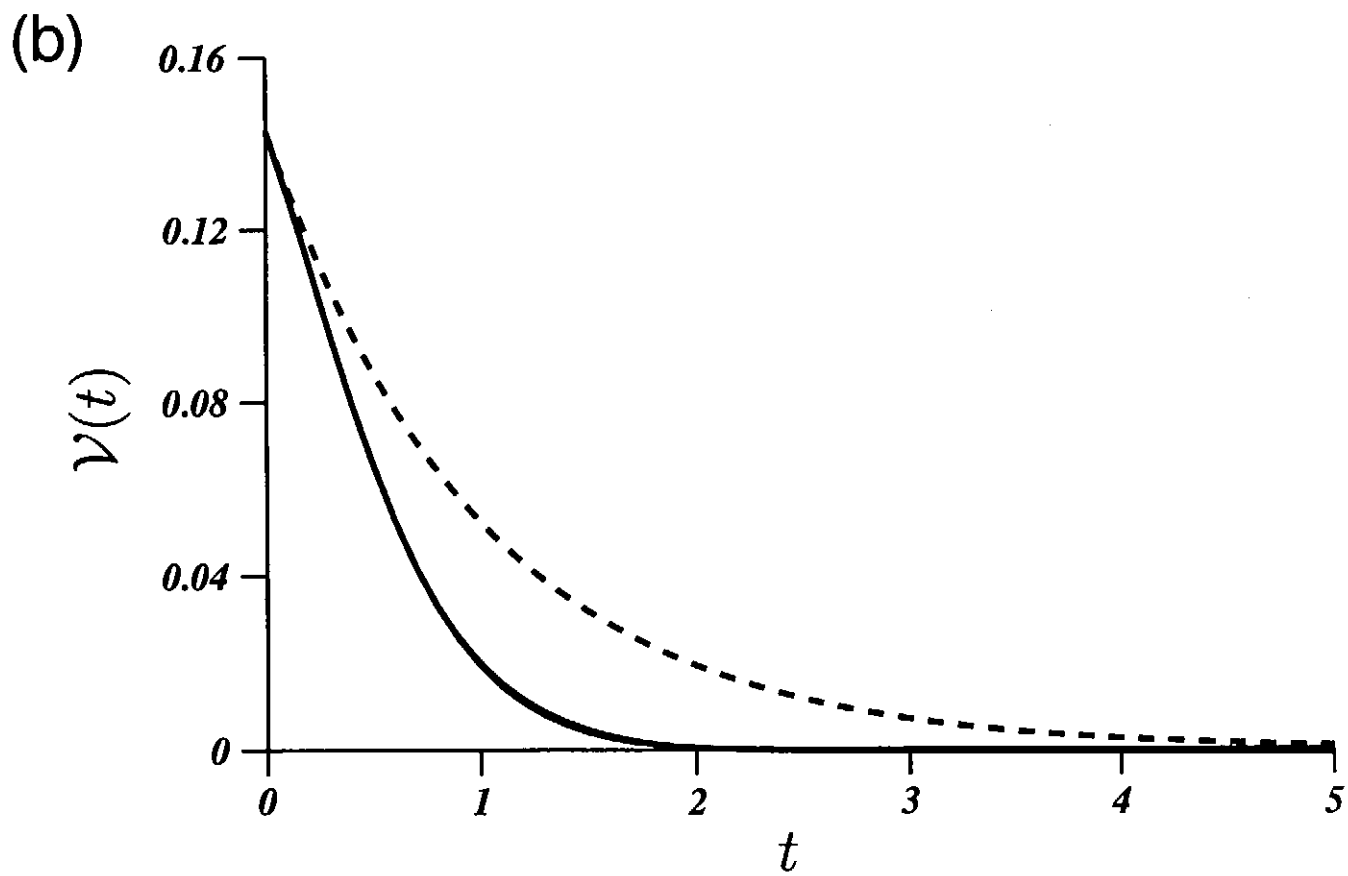
(b)
0.16
0.12
0.08
0.04
0
$\mathcal{V}(t)$
0
1
2
3
4
5
t

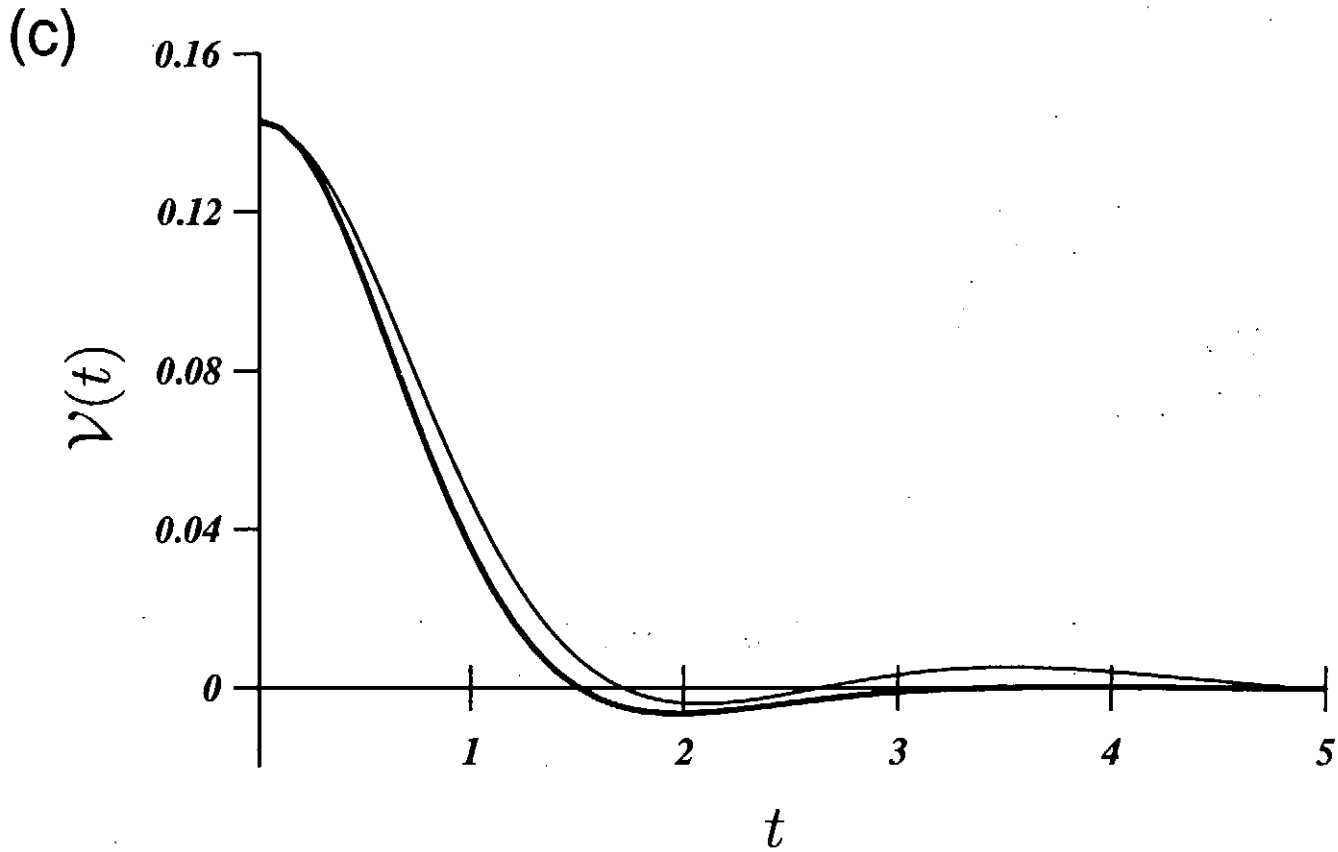
(c)
0.16
0.12
0.08
0.04
0
$\mathcal{V}(t)$
1
2
3
4
5
t

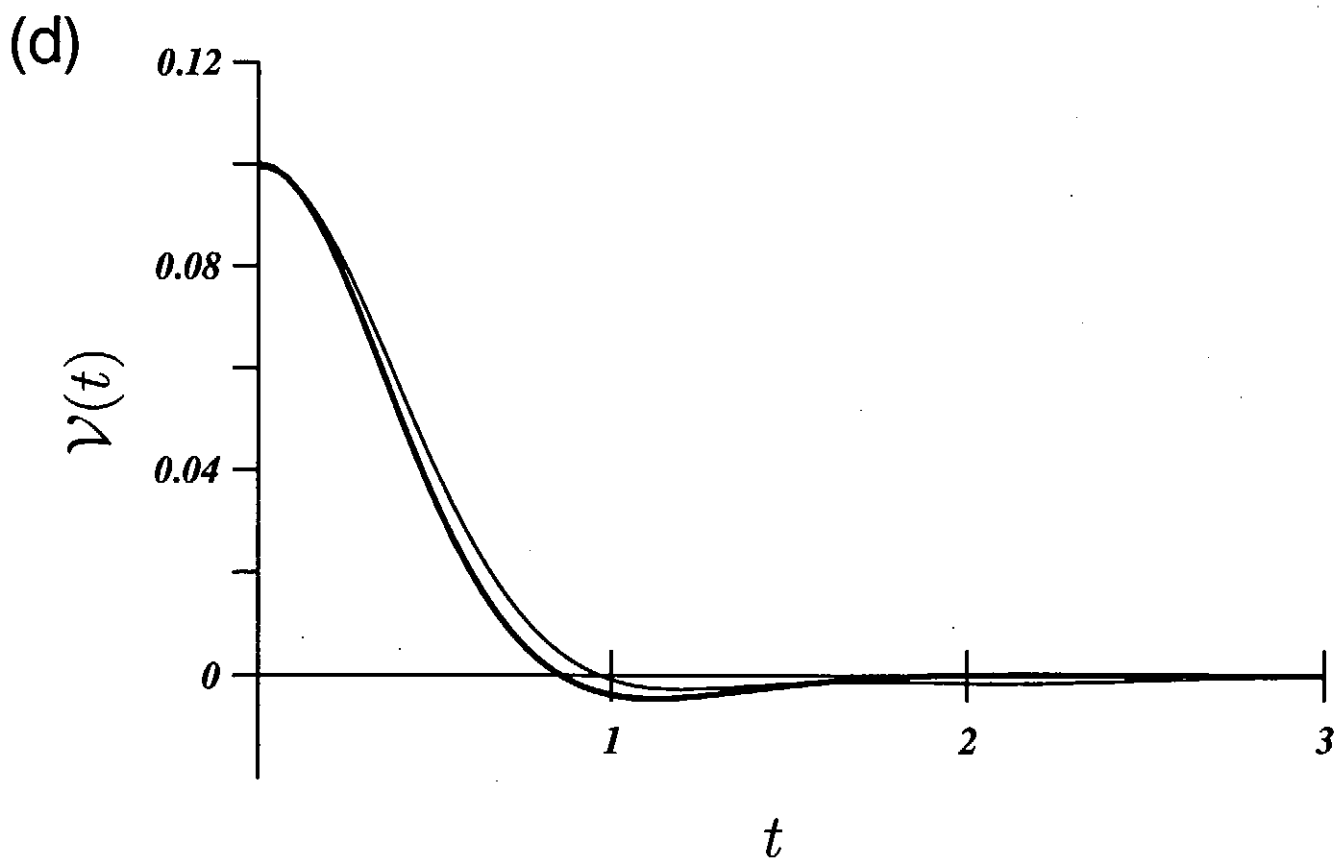
(d)
0.12
0.08
0.04
0
$\mathcal{V}(t)$
1
2
3
t

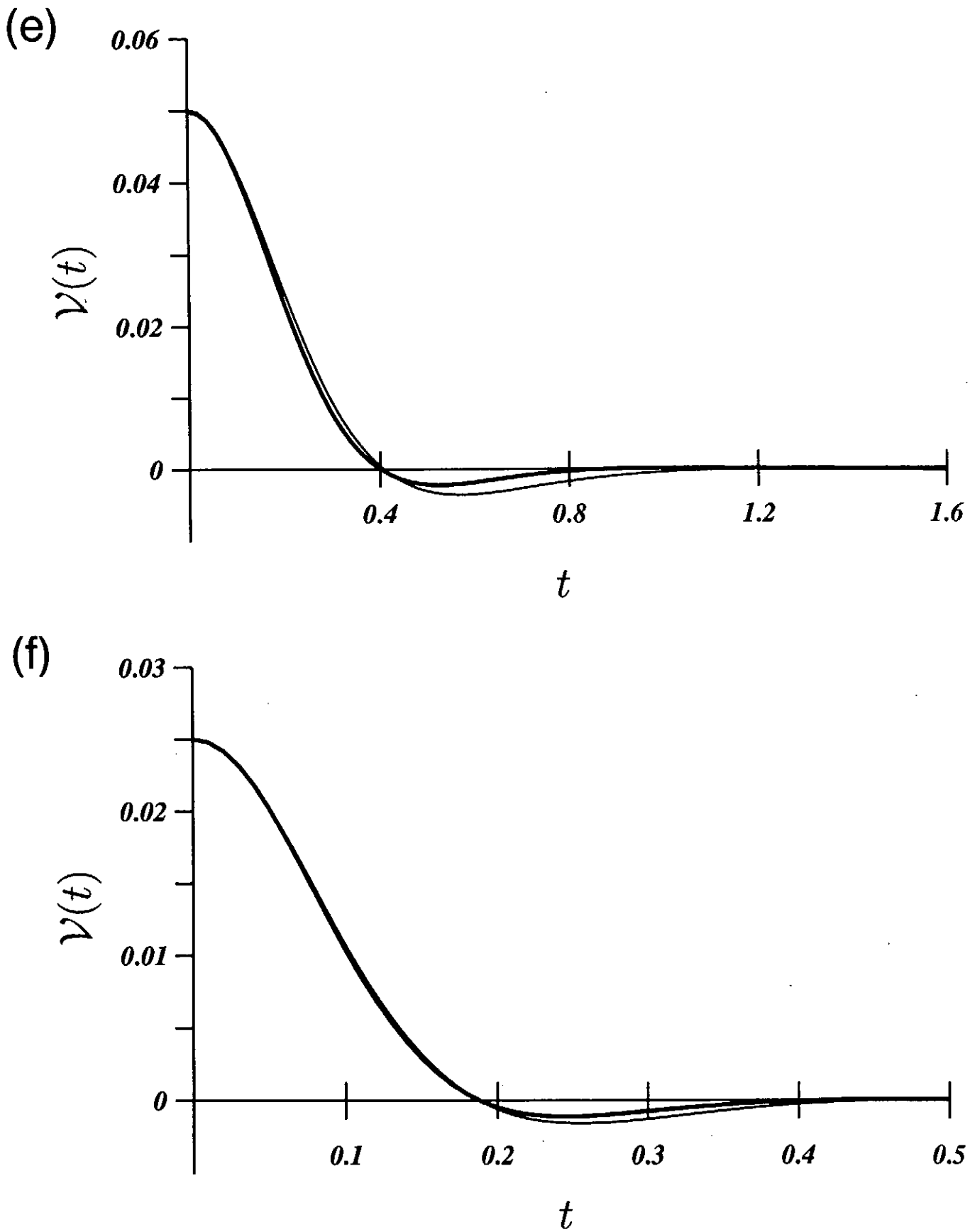

Fig.4 Comparisons between the predictions by the DIA equations (thick solid line) and the evaluations by the direct numerical simulation (thin solid line). The broken lines in (a) and (b) represent the linear solution $\mathcal{V}(\tau) = \mathcal{V}(0)\ \exp[\,-\nu\tau\,]$. (a) $(N, \nu) = (7, 10)$. (b) $(7, 1)$. (c) $(7, 0)$. (d) $(10, 0)$. (e) $(20, 0)$. (f) $(40, 0)$. The agreements are excellent in the cases of $\nu \gg 1$ or $N \gg 1$.

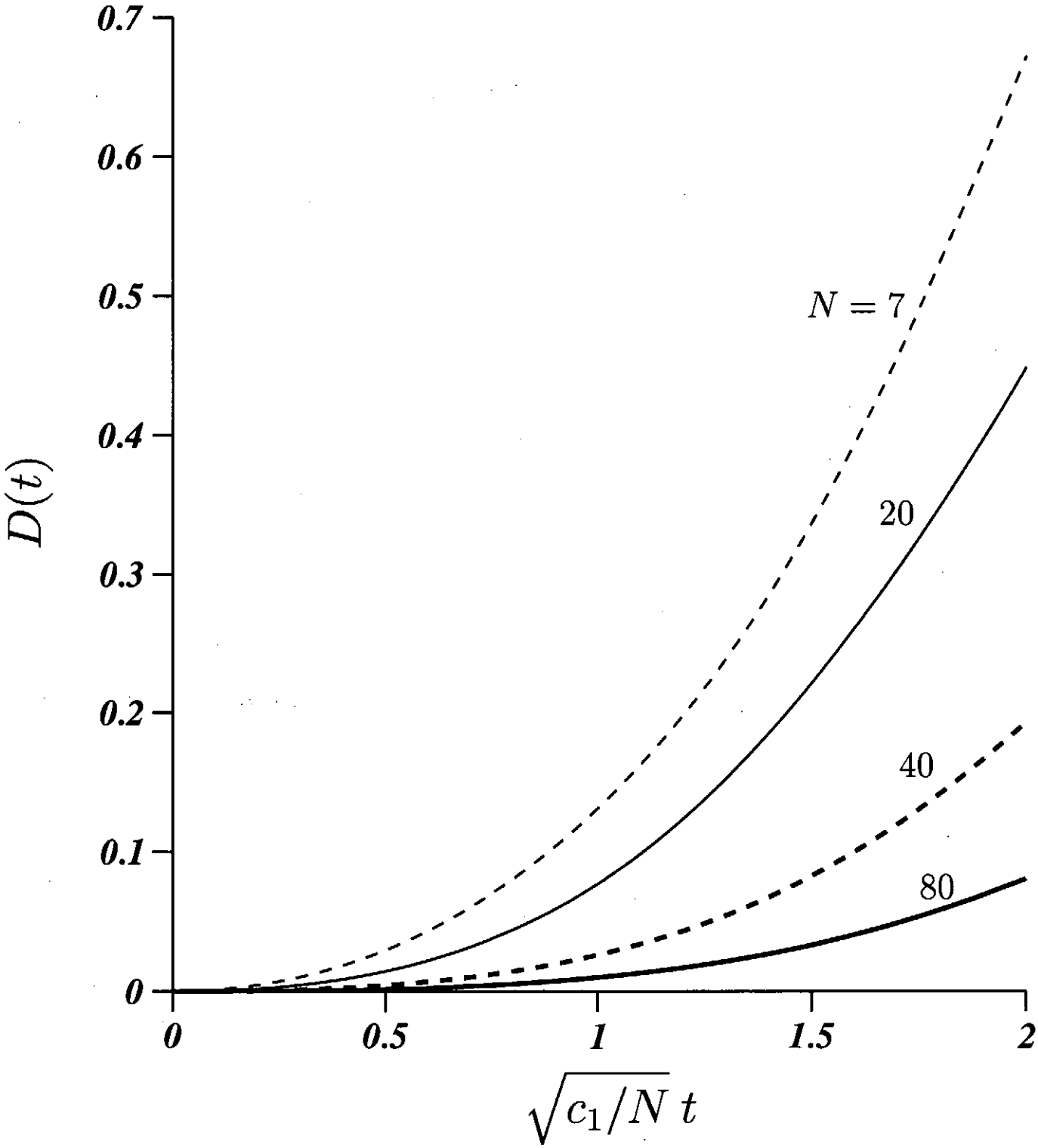

Fig.5 Magnitude of the DI field with $(i_0, j_0, k_0) = (1, 2, 4)$ in the case of $\nu = 0$. The horizontal axis represents the time normalized by decaying time-scale of the auto-correlation function $V_{ii}(t, t')$ (cf. Fig.3(b)). $N = 7$ (thin broken line), 20 (thin solid line), 40 (thick broken line) and 80 (thick solid line).

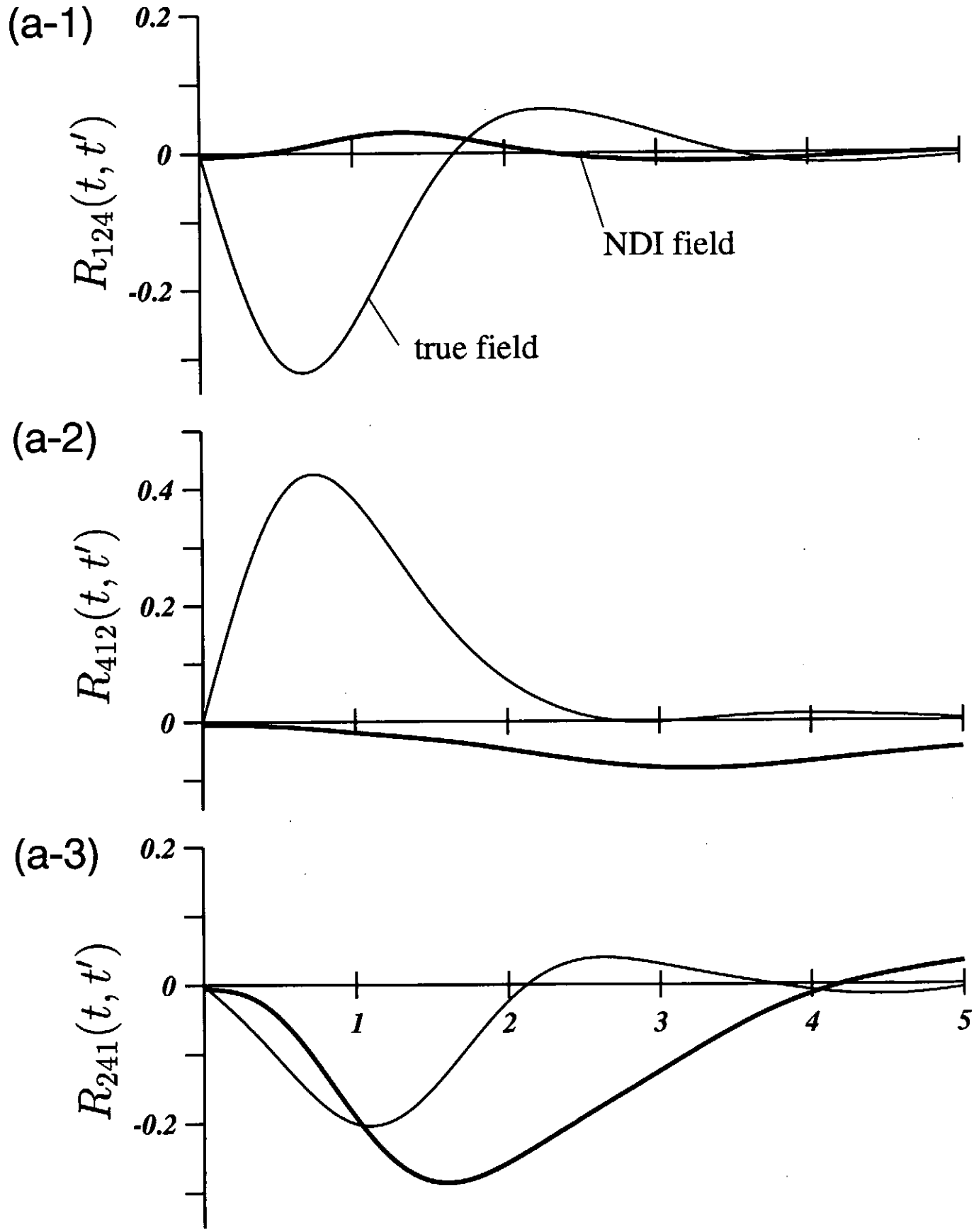
(a-1)
0.2
0
-0.2
$R_{124}(t,t')$
NDI field
true field
(a-2)
0.4
0.2
0
$R_{412}(t,t')$
(a-3)
0.2
0
-0.2
$R_{241}(t,t')$
1
2
3
4
5
$t-t'$

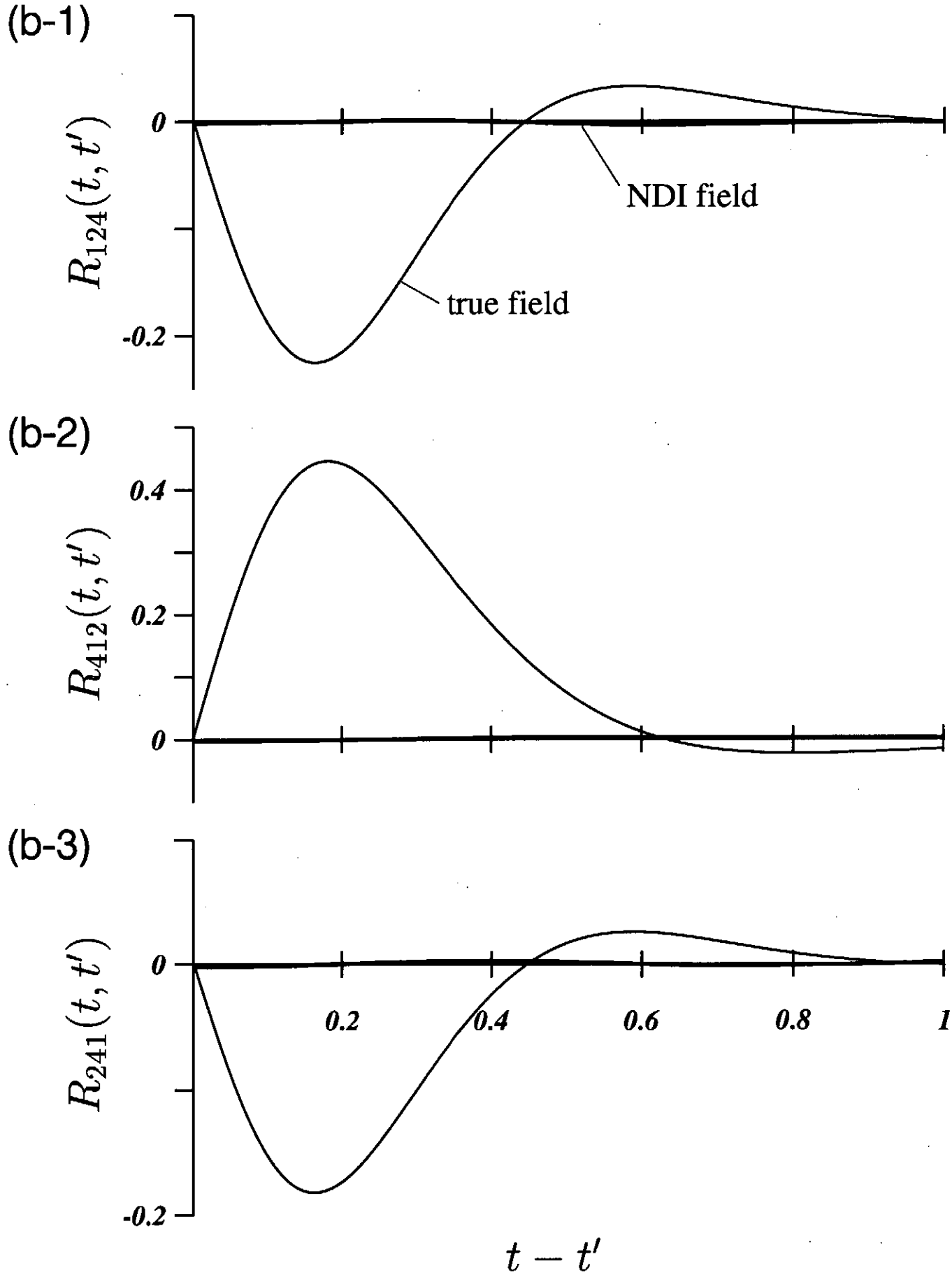

Fig.6 Triple correlation factor R_{ijk} in the true field X_i (thin line) and in the DI field $X_{i/124}$ (thick line) in the weak nonlinear coupling case. (a) $N = 7$. (b) $N = 20$. DIA assumption 2(I) is satisfied well for $N = 20$, but not for $N = 7$.

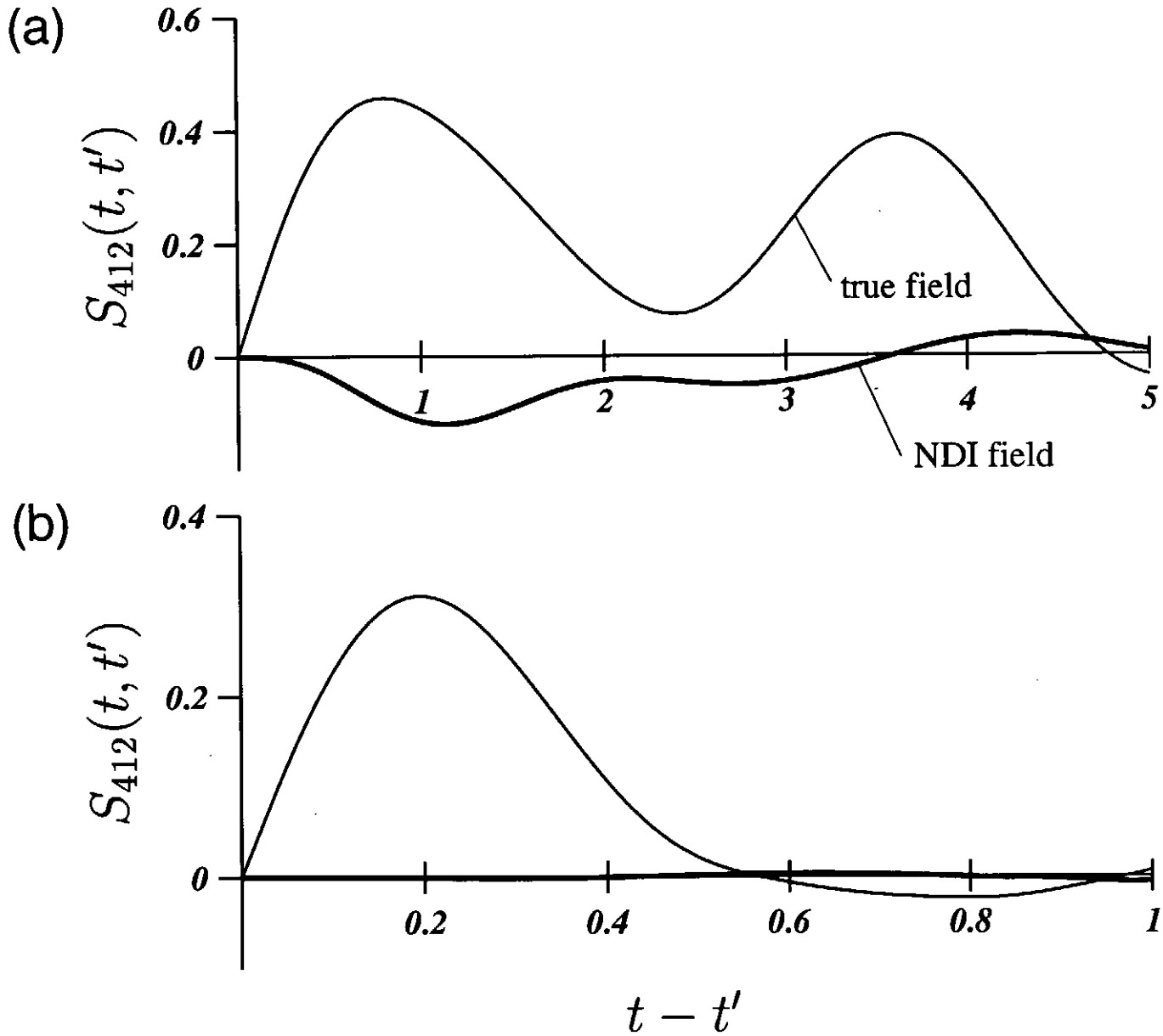

Fig.7 Correlation factor S_{412} in the true field G_{ij} (thin line) and in the NDI field $G^{(0)}_{ij/124}$ (thick line) in the weak nonlinear coupling case. (a) $N = 7$. (b) $N = 20$. DIA assumption 2(II) is satisfied well for $N = 20$, but not for $N = 7$.

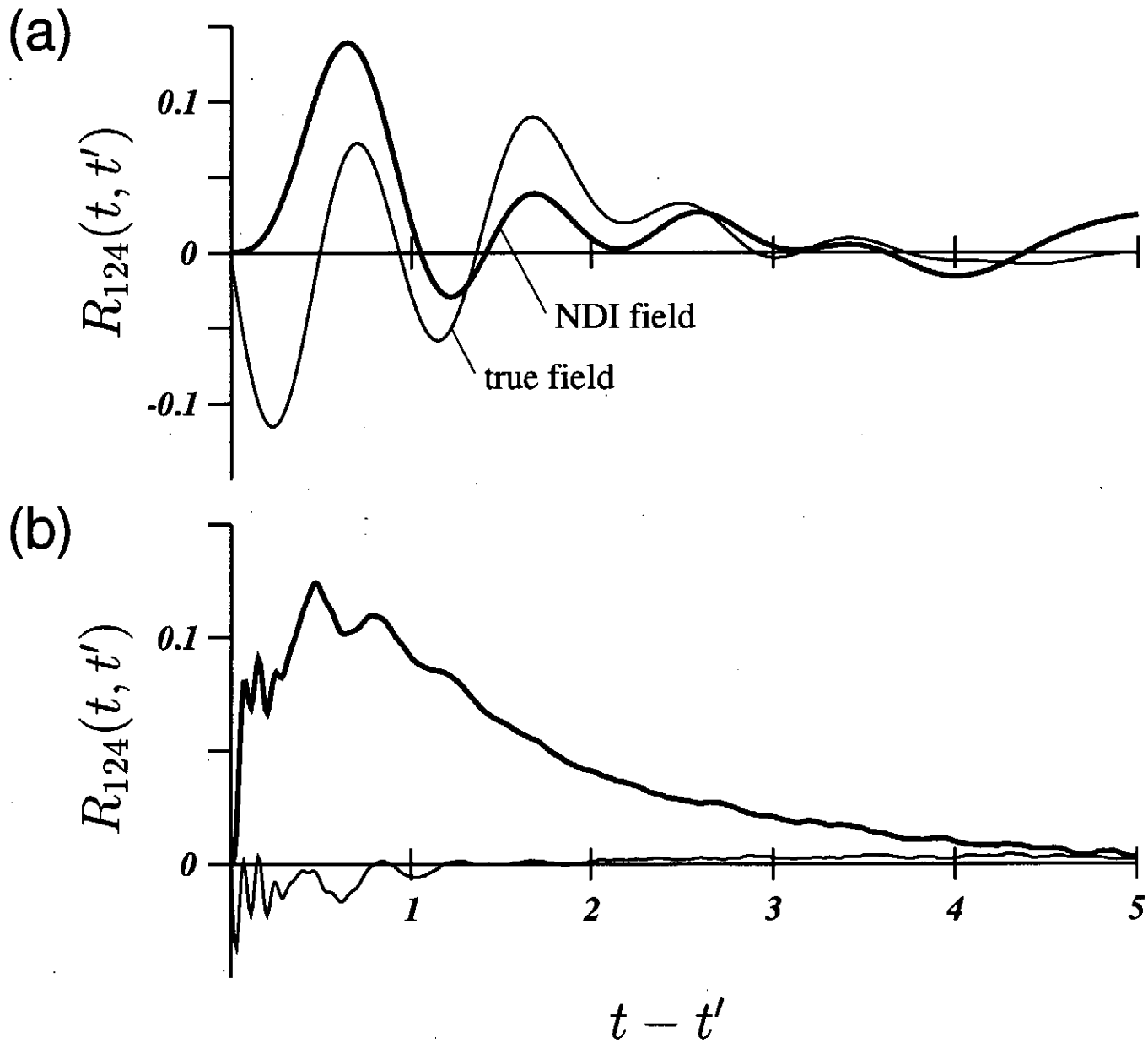

Fig.8 Same as Fig.6 in the strong nonlinear coupling case. DIA assumption 2(I) is not satisfied even for large N.

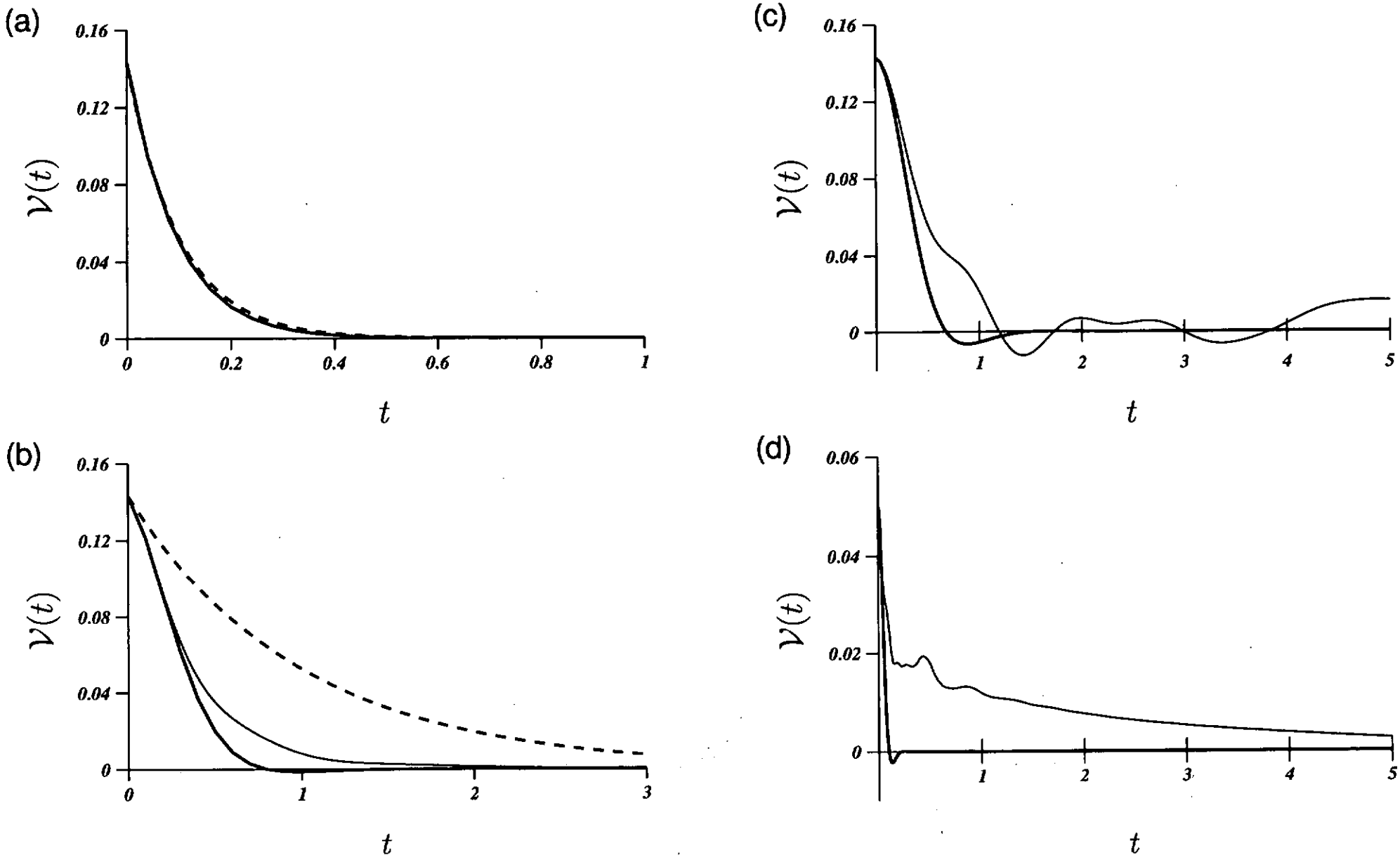

Fig.9 Same as Fig.4 in the strong nonlinear coupling case. (a) $(N,\nu)=(7,10)$. (b) $(N,\nu)=(7,1)$. (c) $(N,\nu)=(7,0)$. (d) $(N,\nu)=(20,0)$.

Recent Issues of NIFS Series

NIFS-453 A. Iiyoshi,
Overview of Helical Systems; Sep. 1996 (IAEA-CN-64/O1-7)

NIFS-454 S. Saito, Y. Nomura, K. Hirose and Y.H. Ichikawa,
Separatrix Reconnection and Periodic Orbit Annihilation in the Harper Map; Oct. 1996

NIFS-455 K. Ichiguchi, N. Nakajima and M. Okamoto,
Topics on MHD Equilibrium and Stability in Heliotron / Torsatron; Oct. 1996

NIFS-456 G. Kawahara, S. Kida, M. Tanaka and S. Yanase,
Wrap, Tilt and Stretch of Vorticity Lines around a Strong Straight Vortex Tube in a Simple Shear Flow; Oct. 1996

NIFS-457 K. Itoh, S.- I. Itoh, A. Fukuyama and M. Yagi,
Turbulent Transport and Structural Transition in Confined Plasmas; Oct. 1996

NIFS-458 A. Kageyama and T. Sato,
Generation Mechanism of a Dipole Field by a Magnetohydrodynamic Dynamo; Oct. 1996

NIFS-459 K. Araki, J. Mizushima and S. Yanase,
The Non-axisymmetric Instability of the Wide-Gap Spherical Couette Flow; Oct. 1996

NIFS-460 Y. Hamada, A. Fujisawa, H. Iguchi, A. Nishizawa and Y. Kawasumi,
A Tandem Parallel Plate Analyzer; Nov. 1996

NIFS-461 Y. Hamada, A. Nishizawa, Y. Kawasumi, A. Fujisawa, K. Narihara, K. Ida, A. Ejiri, S. Ohdachi, K. Kawahata, K. Toi, K. Sato, T. Seki, H. Iguchi, K. Adachi, S. Hidekuma, S.Hirokura, K. Iwasaki, T. Ido, M. Kojima, J. Koong, R. Kumazawa, H. Kuramoto, T. Minami, I. Nomura, H. Sakakita, M. Sasao, K.N. Sato, T. Tsuzuki, J. Xu, I. Yamada and T. Watari,
Density Fluctuation in JIPP T-IIU Tokamak Plasmas Measured by a Heavy Ion Beam Probe; Nov. 1996

NIFS-462 N. Katsuragawa, H. Hojo and A. Mase,
Simulation Study on Cross Polarization Scattering of Ultrashort-Pulse Electromagnetic Waves; Nov. 1996

NIFS-463 V. Voitsenya, V. Konovalov, O. Motojima, K. Narihara, M. Becker and B. Schunke,
Evaluations of Different Metals for Manufacturing Mirrors of Thomson Scattering System for the LHD Divertor Plasma; Nov. 1996

NIFS-464 M. Pereyaslavets, M. Sato, T. Shimozuma, Y. Takita, H. Idei, S. Kubo, K. Ohkubo and K. Hayashi,

Development and Simulation of RF Components for High Power Millimeter Wave Gyrotrons; Nov. 1996

NIFS-465 V.S. Voitsenya, S. Masuzaki, O. Motojima, N. Noda and N. Ohyabu,
On the Use of CX Atom Analyzer for Study Characteristics of Ion Component in a LHD Divertor Plasma; Dec. 1996

NIFS-466 H. Miura and S. Kida,
Identification of Tubular Vortices in Complex Flows; Dec. 1996

NIFS-467 Y. Takeiri, Y. Oka, M. Osakabe, K. Tsumori, O. Kaneko, T. Takanashi, E. Asano, T. Kawamoto, R. Akiyama and T. Kuroda,
Suppression of Accelerated Electrons in a High-current Large Negative Ion Source; Dec. 1996

NIFS-468 A. Sagara, Y. Hasegawa, K. Tsuzuki, N. Inoue, H. Suzuki, T. Morisaki, N. Noda, O. Motojima, S. Okamura, K. Matsuoka, R. Akiyama, K. Ida, H. Idei, K. Iwasaki, S. Kubo, T. Minami, S. Morita, K. Narihara, T. Ozaki, K. Sato, C. Takahashi, K. Tanaka, K. Toi and I. Yamada,
Real Time Boronization Experiments in CHS and Scaling for LHD; Dec. 1996

NIFS-469 V.L. Vdovin, T.Watari and A. Fukuyama,
3D Maxwell-Vlasov Boundary Value Problem Solution in Stellarator Geometry in Ion Cyclotron Frequency Range (final report); Dec. 1996

NIFS-470 N. Nakajima, M. Yokoyama, M. Okamoto and J. Nührenberg,
Optimization of M=2 Stellarator; Dec. 1996

NIFS-471 A. Fujisawa, H. Iguchi, S. Lee and Y. Hamada,
Effects of Horizontal Injection Angle Displacements on Energy Measurements with Parallel Plate Energy Analyzer; Dec. 1996

NIFS-472 R. Kanno, N. Nakajima, H. Sugama, M. Okamoto and Y. Ogawa,
Effects of Finite-β and Radial Electric Fields on Neoclassical Transport in the Large Helical Device; Jan. 1997

NIFS-473 S. Murakami, N. Nakajima, U. Gasparino and M. Okamoto,
Simulation Study of Radial Electric Field in CHS and LHD; Jan. 1997

NIFS-474 K. Ohkubo, S. Kubo, H. Idei, M. Sato, T. Shimozuma and Y. Takita,
Coupling of Tilting Gaussian Beam with Hybrid Mode in the Corrugated Waveguide; Jan. 1997

NIFS-475 A. Fujisawa, H. Iguchi, S. Lee and Y. Hamada,
Consideration of Fluctuation in Secondary Beam Intensity of Heavy Ion Beam Prove Measurements; Jan. 1997

NIFS-476 Y. Takeiri, M. Osakabe, Y. Oka, K. Tsumori, O. Kaneko, T. Takanashi, E. Asano, T. Kawamoto, R. Akiyama and T. Kuroda,

Long-pulse Operation of a Cesium-Seeded High-Current Large Negative Ion Source; Jan. 1997

NIFS-477 H. Kuramoto, K. Toi, N. Haraki, K. Sato, J. Xu, A. Ejiri, K. Narihara, T. Seki, S. Ohdachi, K. Adati, R. Akiyama, Y. Hamada, S. Hirokura, K. Kawahata and M. Kojima,
Study of Toroidal Current Penetration during Current Ramp in JIPP T-IIU with Fast Response Zeeman Polarimeter; Jan., 1997

NIFS-478 H. Sugama and W. Horton,
Neoclassical Electron and Ion Transport in Toroidally Rotating Plasmas; Jan. 1997

NIFS-479 V.L. Vdovin and I.V. Kamenskij,
3D Electromagnetic Theory of ICRF Multi Port Multi Loop Antenna; Jan. 1997

NIFS-480 W.X. Wang, M. Okamoto, N. Nakajima, S Murakami and N. Ohyabu,
Cooling Effect of Secondary Electrons in the High Temperature Divertor Operation; Feb. 1997

NIFS-481 K. Itoh, S.-I. Itoh, H. Soltwisch and H.R. Koslowski,
Generation of Toroidal Current Sheet at Sawtooth Crash; Feb. 1997

NIFS-482 K. Ichiguchi,
Collisionality Dependence of Mercier Stability in LHD Equilibria with Bootstrap Currents; Feb. 1997

NIFS-483 S. Fujiwara and T. Sato,
Molecular Dynamics Simulations of Structural Formation of a Single Polymer Chain: Bond-orientational Order and Conformational Defects; Feb. 1997

NIFS-484 T. Ohkawa,
Reduction of Turbulence by Sheared Toroidal Flow on a Flux Surface; Feb. 1997

NIFS-485 K. Narihara, K. Toi, Y. Hamada, K. Yamauchi, K. Adachi, I. Yamada, K. N. Sato, K. Kawahata, A. Nishizawa, S. Ohdachi, K. Sato, T. Seki, T. Watari, J. Xu, A. Ejiri, S. Hirokura, K. Ida, Y. Kawasumi, M. Kojima, H. Sakakita, T. Ido, K. Kitachi, J. Koog and H. Kuramoto,
Observation of Dusts by Laser Scattering Method in theJIPPT-IIU Tokamak Mar. 1997

NIFS-486 S. Bazdenkov, T. Sato and The Complexity Simulation Group,
Topological Transformations in Isolated Straight Magnetic Flux Tube; Mar. 1997

NIFS-487 M. Okamoto,
Configuration Studies of LHD Plasmas; Mar. 1997

NIFS-488 A. Fujisawa, H. Iguchi, H. Sanuki, K. Itoh, S. Lee, Y. Hamada, S. Kubo, H. Idei, R. Akiyama, K. Tanaka, T. Minami, K. Ida, S. Nishimura, S. Morita, M. Kojima, S. Hidekuma, S.-I. Itoh, C. Takahashi, N. Inoue, H. Suzuki, S. Okamura and K. Matsuoka,
Dynamic Behavior of Potential in the Plasma Core of the CHS Heliotron/Torsatron; Apr. 1997

NIFS-489 T. Ohkawa,
Pfirsch - Schlüter Diffusion with Anisotropic and Nonuniform Superthermal Ion Pressure; Apr. 1997

NIFS-490 S. Ishiguro and The Complexity Simulation Group,
Formation of Wave-front Pattern Accompanied by Current-driven Electrostatic Ion-cyclotron Instabilities; Apr. 1997

NIFS-491 A. Ejiri, K. Shinohara and K. Kawahata,
An Algorithm to Remove Fringe Jumps and its Application to Microwave Reflectometry; Apr. 1997

NIFS-492 K. Ichiguchi, N. Nakajima, M. Okamoto,
Bootstrap Current in the Large Helical Device with Unbalanced Helical Coil Currents; Apr. 1997

NIFS-493 S. Ishiguro, T. Sato, H. Takamaru and The Complexity Simulation Group,
V-shaped dc Potential Structure Caused by Current-driven Electrostatic Ion-cyclotron Instability; May 1997

NIFS-494 K. Nishimura, R. Horiuchi, T. Sato,
Tilt Stabilization by Energetic Ions Crossing Magnetic Separatrix in Field-Reversed Configuration; June 1997

NIFS-495 T. -H. Watanabe and T. Sato,
Magnetohydrodynamic Approach to the Feedback Instability; July 1997

NIFS-496 K. Itoh, T. Ohkawa, S. -I.Itoh, M. Yagi and A. Fukuyama
Suppression of Plasma Turbulence by Asymmetric Superthermal Ions; July 1997

NIFS-497 T. Takahashi, Y. Tomita, H. Momota and Nikita V. Shabrov,
Collisionless Pitch Angle Scattering of Plasma Ions at the Edge Region of an FRC; July 1997

NIFS-498 M. Tanaka, A.Yu Grosberg, V.S. Pande and T. Tanaka,
Molecular Dynamics and Structure Organization inStrongly-Coupled Chain of Charged Particles; July 1997

NIFS-499 S. Goto and S. Kida,
Direct-interaction Approximation and Reynolds-number Reversed Expansion for a Dynamical System; July 1997